PHYSICAL SCIENCES

A skin-mimicking multifunctional hydrogel via hierarchical, reversible noncovalent interactions

Xingkui Guo[1], Songlin Zhang[2]*, Shubham Patel[3], Xiaolu Sun[4], You-Liang Zhu[5], Zechang Wei[1], Rongguo Wang[4], Xiaodong He[4], Zuankai Wang[6,7]*, Cunjiang Yu[3]*, Swee Ching Tan[1]*

Artificial skin is essential for bionic robotics, facilitating human skin–like functions such as sensation, communication, and protection. However, replicating a skin-matched all-in-one material with excellent mechanical properties, self-healing, adhesion, and multimodal sensing remains a challenge. Herein, we developed a multifunctional hydrogel by establishing a consolidated organic/metal bismuth ion architecture (COMBIA). Benefiting from hierarchical reversible noncovalent interactions, the COMBIA hydrogel exhibits an optimal combination of mechanical and functional properties, particularly its integrated mechanical properties, including unprecedented stretchability, fracture toughness, and resilience. Furthermore, these hydrogels demonstrate superior conductivity, optical transparency, freezing tolerance, adhesion capability, and spontaneous mechanical and electrical self-healing. These unified functions render our hydrogel exceptional properties such as shape adaptability, skin-like perception, and energy harvesting capabilities. To demonstrate its potential applications, an artificial skin using our COMBIA hydrogel was configured for stimulus signal recording, which, as a promising soft electronics platform, could be used for next-generation human-machine interfaces.

INTRODUCTION

Multiple arduous functions (i.e., mechanical robustness, self-healing, proprioception, etc.) of biological skins have been well integrated through evolution, and their unique multifunctional characteristics can not only provide protection but also mediate interactions with the world (*1*). Electronic skin (e-skin), which mimics the structures and functions of biological skins, enables the realization of skin-like features with extensive applications in human-machine interfaces, soft robotics, and biomedical prosthetics (*2*). However, biological systems are inherently intelligent, whereas electronic systems are artificially intelligent. These two types of systems are fundamentally distinct and incompatible. Considerable efforts have been made to recreate the properties of biological skins (*3*, *4*). Nevertheless, a convergent system that has combined functions that are mutually exclusive (i.e., high resilience/high toughness, self-adhesion/high toughness, and self-healing/high toughness) still cannot be achieved with conventional strategies that are physically or chemically complicated (*5*, *6*). For instance, physically compositing conductive materials (i.e., liquid metals, thin metal films, and arrays of organic field-effect transistors) with polymer elastomers is associated with unsatisfactory interfaces or poor biocompatibility (*7*, *8*). Chemically synthesized nanoconductive materials (i.e., carbon nanotubes and graphene, metal nanowires, and conducting polymers) suffer from structural heterogeneity or complex in-line synthesis (*9*, *10*).

Hydrogels are promising alternative e-skin materials owing to their excellent biocompatibility, tunable conducting sensing channels, strong mechanical compliance, and low interfacial resistance (*11*–*13*). Several advantages of biological skins are recreated via different hydrogel materials, including stretchability, self-healing, self-adhesion, etc. Nevertheless, few of these studies are comparable to the functions of biological skins as an all-in-one material, for instance, suitable mechanical strength but poor toughness or resilience, or high toughness but no antifreezing or self-adhesion or self-healing ability (*14*–*17*). These limitations stem from the fundamental conflict between mechanical robustness and dynamic functionality. High toughness typically relies on strong covalent or physical cross-linking, which resists deformation but restricts network reorganization, thereby impairing resilience, self-healing, and adhesion (*18*, *19*). Conversely, dynamic properties depend on weak interactions that facilitate self-recovery but weaken overall toughness (*20*). In addition, the introduction of dense cross-linking further restricts molecular mobility, making it difficult to achieve a synergistic balance of these properties (*21*). The use of metal ions or ionic liquids as additives, which are among the most promising strategies for recreating hydrogels with a unique combination of functions, can endow hydrogels with increased conductivity, freezing resistance, and mechanical performance. However, the intrinsic limitations of traditional ion-polymer networks, such as opacity, toxicity, leakiness, weak coordination, and poor miscibility, impede their application in the production of multifunctional hydrogels (*22*–*25*). Consequently, seamlessly integrating heterogeneous functions into an all-in-one material similar to biological skins remains an unresolved challenge.

Herein, we report a consolidated organic-metal ion architecture within zwitterionic polymer networks (Fig. 1), constructed through a facile supramolecular network manipulation process. Briefly, our

[1]Department of Materials Science and Engineering, National University of Singapore, Singapore 117574, Singapore. [2]State Key Laboratory of Molecular Engineering of Polymers, Department of Macromolecular Science, Institute of Fiber Materials and Devices, and Laboratory of Advanced Materials, Fudan University, Shanghai 200438, China. [3]The Grainger College of Engineering, Department of Electrical and Computer Engineering, Department of Materials Science and Engineering, Department of Mechanical Science and Engineering, Departments of Bioengineering, The Grainger College of Engineering, Beckman Institute for Advanced Science and Technology, Materials Research Laboratory, Nick Holonyak Micro and Nanotechnology Laboratory, University of Illinois, Urbana-Champaign, Urbana, IL 61801, USA. [4]National Key Laboratory of Science and Technology on Advanced Composites in Special Environments, Harbin Institute of Technology, Harbin 150080, P. R. China. [5]State Key Laboratory of Supramolecular Structure and Materials, College of Chemistry, Jilin University, Changchun, China. [6]Department of Mechanical Engineering, The Hong Kong Polytechnic University, Hong Kong SAR, P. R. China. [7]Shenzhen Research Institute of The Hong Kong Polytechnic University, Shenzhen, P. R. China.
*Corresponding author. Email: zhangsonglin@fudan.edu.cn (S.Z.); zk.wang@polyu.edu.hk (Z.W.); cunjiang@illinois.edu (C.Y.); msetansc@nus.edu.sg (S.C.T.)

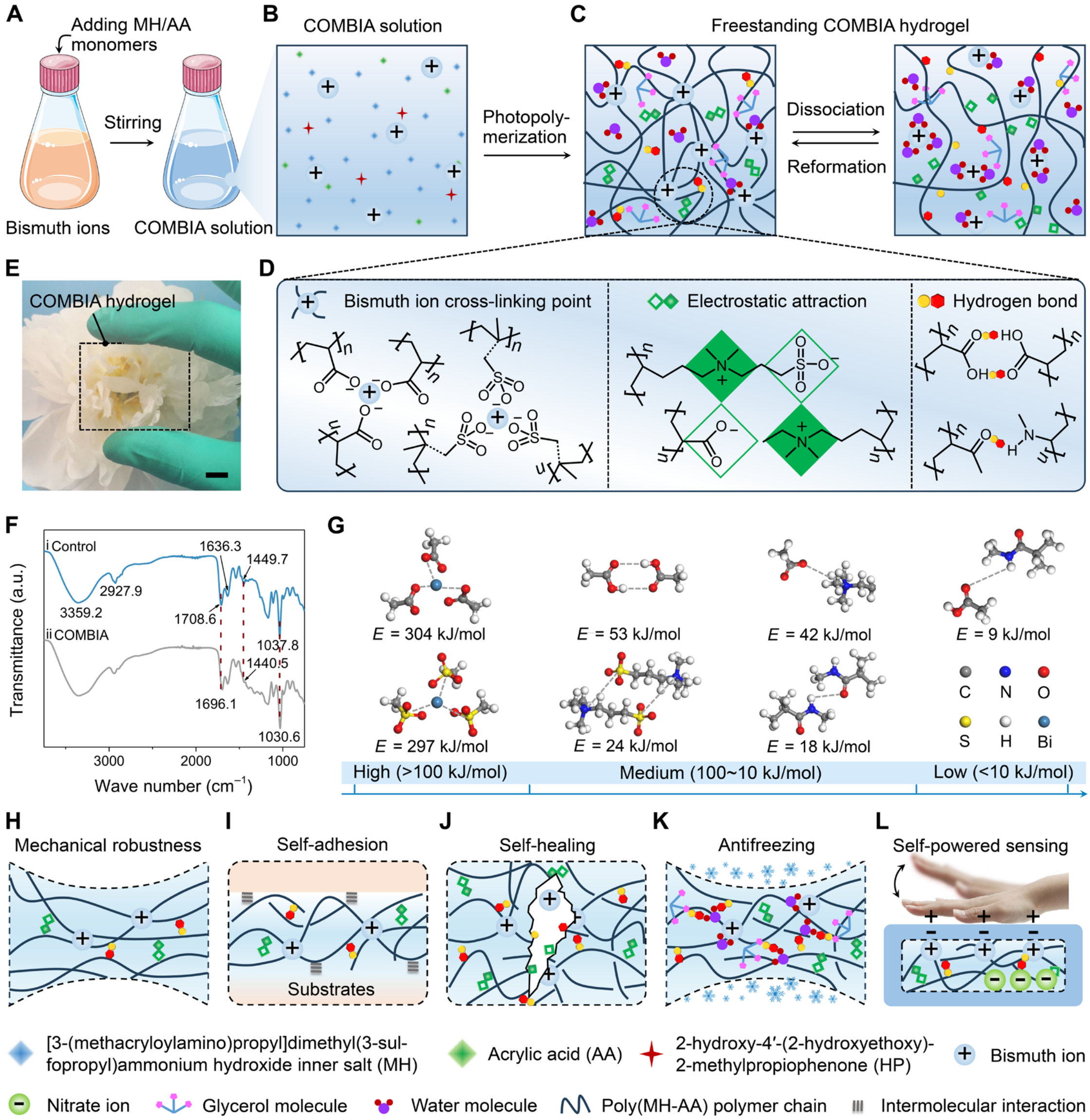

Fig. 1. Schematic of the all-in-one COMBIA hydrogel. (**A** to **C**) Preparation of COMBIA hydrogels, including the COMBIA solution (A) and the transformation from a liquid mixture to a solid freestanding hydrogel via a photopolymerization approach [(B) and (C)]. (**D**) Schematic of primary molecular interactions within the COMBIA architecture. (**E**) A 2-mm–thick COMBIA hydrogel film (size: 4 cm by 5 cm) was placed on a blooming flower (scale bar, 1 cm). (**F**) FTIR spectra of the (i) control and (ii) COMBIA hydrogels. a.u., arbitrary units. (**G**) Binding energies of hierarchical interactions in the COMBIA architecture. (**H** to **L**) Schematic showing various properties of COMBIA hydrogels, including mechanical robustness (H), self-adhesion (I), self-healing (J), freezing resistance (K), and self-powered sensing (L).

functional hydrogel was prepared by polymerizing an ammonium hydroxide inner salt and an unsaturated acrylic-based monomer in a water/glycerol binary solvent containing bismuth ions. Owing to the hierarchical multiple reversible noncovalent interactions, hydrogels with a consolidated organic/metal bismuth ion architecture (referred to as COMBIA) demonstrated a hierarchically dynamically cross-linked network, ranging from low to high in energy scale, among various functional groups (i.e., carboxyl, amino, and zwitterionic groups) within neighboring polymer chains. Notably, bismuth ions play a vital role in manipulating the structure of COMBIA because of their unique structural and functional properties [i.e., colorlessness (*26*), nontoxicity (*27*), high coordination ability (*28*), and excellent structural stability (*29*)]. Accordingly, the resultant hydrogel displayed ultrahigh stretchability (5417%), desirable tensile strength (0.37 MPa), prominent fracture toughness (12.14 MJ m^{-3}), skin-like Young's modulus (128.3 kPa), strong resilience (92.36%), excellent adhesion (44.7 kPa), and spontaneous self-healing. Furthermore, the hydrogel also exhibited high ionic conductivity (7.52 S m^{-1}), good antifreezing resistance (−32.27°C), great optical transparency (>97.46% in visible light), and moisture preservation. Given these merits, we configured a self-powered e-skin using our hydrogel that demonstrated highly stable and reliable sensing signals. In summary, this study elucidated the broad applicability of COMBIA as a single homogeneous material platform, opening a promising avenue for the fabrication of versatile gel platforms for more integrated intelligent wearable sensors.

RESULTS

Design of COMBIA hydrogels

The COMBIA hydrogel was designed by creating a bismuth ion–coordinated supramolecular framework with hierarchical multiple reversible noncovalent interactions (Fig. 1, A to D). Specifically, we developed a synthetic protocol based on the copolymerization of [3-(methacryloylamino)propyl]dimethyl(3-sulfopropyl)ammonium hydroxide inner salt (MH) and acrylic acid (AA) in the presence of trivalent transition metal bismuth ions (Fig. 1, A to C). Among these components, zwitterionic polymer chains produced by MH/AA copolymerization function as soft segments to provide abundant functional sites (i.e., $-N^+(CH_3)-$, $-SO_3^-$, $-COO^-$, and –N–H). This contributes to the formation of hierarchical multiple reversible physical interactions owing to their distinct cross-linking kinetics, thus obtaining desirable properties. For instance, zwitterionic groups along polymer chains can readily form negative and positive ion channels, thus quickly promoting ion transport. Concomitantly, the zwitterionic network endows the hydrogel with strong water-retaining, adhesion, and self-healing properties as a result of the dynamic electrostatic interactions between oppositely charged groups and hydrogen bonding (*30*–*32*). Furthermore, compared with the existing metal ions used for hydrogel fabrication, metal bismuth ions are used as hygroscopic and ionic cross-linking agents owing to their superior advantages, such as transparency, harmlessness, and high coordination capacity. Dynamic metal-ligand coordinate complexes with high binding energies between bismuth ions and active sites can form cross-linking points within polymer networks, substantially enhancing the mechanical properties of the hydrogel. Notably, the addition of bismuth ions also improves the ionic conductivity of these materials. Their multiple dynamic binding energies were calculated via density functional theory (DFT), indicating that, in general, the binding energies within the supramolecular architectures presented hierarchical characteristics across two orders of magnitude in the energy scale, ranging from several to hundreds of kJ/mol (Supplementary Text 1). This feature results in distinctive bonding and rebonding reactions within supramolecular systems during the mechanical deformation process. Therefore, combining zwitterionic polymer chains with kinetically distinct cross-links and bismuth-ligand coordinate complexes can be used to construct COMBIA hydrogels via the manipulation of hierarchical multiple noncovalent interactions (Fig. 1D). The unique reversible characteristics of these interactions can facilitate efficient energy dissipation across multiple scales, enhancing toughness while ensuring rapid recovery and high resilience through the reversibility of the bonds, allowing the material to return to its original state after deformation. Moreover, dynamic interfacial interactions allow for robust adhesion, even in challenging environments like underwater conditions, by overcoming interfacial water accumulation. The inherent reversibility of these interactions also enables autonomous self-healing, allowing the network to spontaneously reform bonds by coordinating the reformation of multiple types of bonds, thereby restoring both mechanical strength and functionality without external intervention. This results in a hydrogel with an unprecedented balance of mechanical strength, resilience, adhesion, and self-healing properties.

An optimal solution with a 1:1.66 MH:AA weight ratio and bismuth ion content of 0.6 wt % was prepared for the COMBIA hydrogel. By increasing the bismuth ion content, the stretchability, toughness, resilience, ionic conductivity, and freezing tolerance of the COMBIA hydrogel can be enhanced. Water/glycerol binary solvents were used as the liquid phase to prevent $Bi(NO_3)_3{\cdot}5H_2O$ precipitation and increase the antifreezing ability. Consequently, an entangled supramolecular architecture comprising metal-ligand coordination combined with zwitterionic structures was readily formed, which is critical for yielding a mechanically robust yet multifunctional COMBIA hydrogel. As shown in Fig. 1E and fig. S1, the COMBIA hydrogel was highly transparent (up to 97.46% at 400 to 800 nm) because of its homogeneous microstructure, such as a uniform interconnected porous structure (pore size ranging from 10 to 50 μm; fig. S2). These interconnected porous structures potentially prevent crack propagation and facilitate the transfer of ions within the hydrogels, which can enhance ionic conductivity of hydrogels (*33*).

The presence of coordination interactions between bismuth ions and polymer chains was confirmed through changes in the chemical environment of the $-COO^-$ and $-SO_3^-$ functional groups via Fourier transform infrared (FTIR) spectroscopy (Fig. 1F and Supplementary Text 2). The red shift of the characteristic peaks at 1708.6 (C═O stretching vibration), 1449.7 ($-COO^-$ symmetrical stretching vibration), and 1037.8 cm^{-1} ($-SO_3^-$ symmetrical stretching vibration) indicated intermolecular metal-ligand coordination interactions between Bi^{3+} and $-COO^-/-SO_3^-$. Notably, the x-ray photoelectron spectroscopy (XPS) results were consistent with the above findings (fig. S3). On the basis of DFT calculations (Fig. 1G, fig. S4, and table S1), hierarchical behaviors involving multiple reversible noncovalent interactions within the hydrogel were observed. Among them, –C═O/–N–H (MH/AA) exhibited a low binding energy of 9 kJ/mol, –C═O/–N–H (MH/MH) of 18 kJ/mol, $-N^+(CH_3)-/-SO_3^-$ (MH/MH) of 24 kJ/mol, $-N^+(CH_3)-/-COO^-$ (MH/AA) of 42 kJ/mol, and –C═O/–C–OH (AA/AA) of 53 kJ/mol demonstrated medium binding energies. The combination of medium and low binding energies contributes to structural stability, dynamic tunability, and ion/molecule transport. Upon coordination with bismuth ions, the network system incorporated high binding energies of 297 ($Bi^{3+}/-SO_3^-$) and 304 kJ/mol ($Bi^{3+}/-COO^-$), thereby establishing a strong polymer framework with metal-ligand coordination bonds. High binding energies are associated with increased strength, enhanced functionality, and improved durability. In summary, hierarchical multiple reversible noncovalent interactions based on bismuth coordination bonds synergistically contribute to the construction of a COMBIA hydrogel with integrated functions of high mechanical robustness, self-healing, self-adhesion, antifreezing, and self-powered sensing properties (Fig. 1, H to L).

Mechanical properties of COMBIA hydrogels

The formation of the COMBIA structure resulted in markedly enhanced mechanical properties of our hydrogel, which is of considerable importance for its application as an advanced generation of e-skin. The COMBIA hydrogel with a bismuth ion concentration of 0.6 wt % (i.e., $\gamma = 0.6$) exhibited a tensile strength of 0.37 MPa, which was eight times greater than that of the control hydrogel. Furthermore, elongation at break and toughness were improved by 3.5 times and 39 times (5417% and 12.14 MJ m^{-3}), respectively (Fig. 2, A to C; fig. S5; and movie S1). It is noteworthy that a higher bismuth ion content resulted in more metal-ligand coordinate complexes, necessitating greater energy to deform the polymer chains. This is evidenced by the tensile modulus, with values for the samples at $\gamma = 0$, 0.2, 0.4, 0.6, and 0.8 being 97.6, 104.3, 116.2, 128.3, and 145.4 kPa, respectively. In Fig. 2C, we also note that low and medium interactions were primarily prominent at small strains, whereas high interactions became

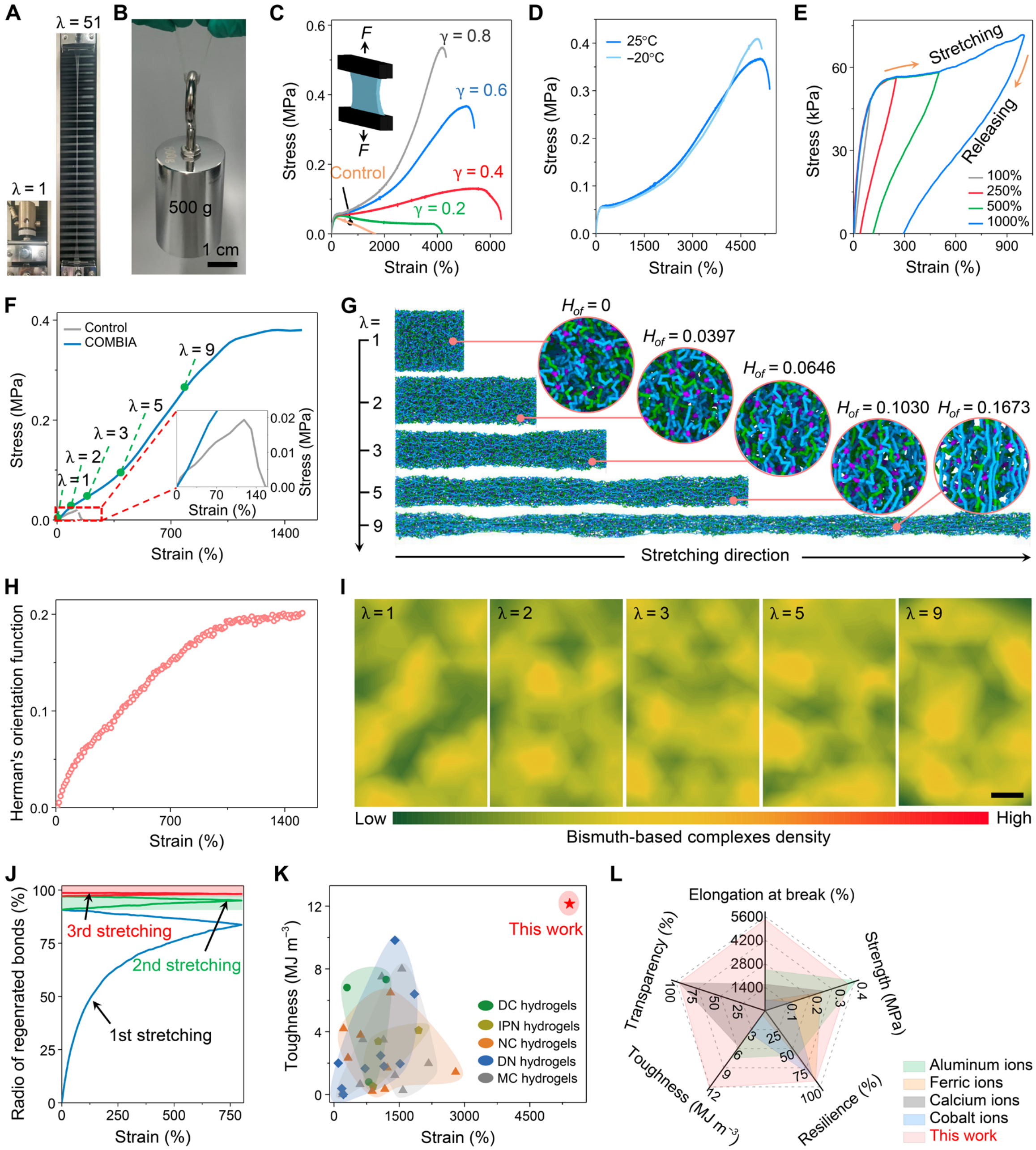

Fig. 2. Mechanical properties of the COMBIA hydrogel. (**A**) Photos of the COMBIA hydrogel in the original state (λ = 1) and highly stretched state (λ = 51) (scale bar, 3 cm). (**B**) Demonstration of the COMBIA hydrogel supporting a 0.5-kg mass (scale bar, 1 cm). (**C**) Effect of the bismuth ion content on the tensile properties of the COMBIA hydrogel films. (**D**) Stress-strain curves of the COMBIA hydrogels at 25 and −20°C. (**E**) Cyclic stretching-releasing from 100 to 1000%. (**F**) Stress-strain curves of the control and COMBIA samples via CG-MD simulation. (**G**) Snapshots of the molecular network of COMBIA at different testing strains (λ). The insets display the polymer chain alignment effect at λ = 1, 2, 3, 5, and 9. (**H**) Evolution of the value of H_{of} over the strain for COMBIA. (**I**) Density distribution of bismuth-based complexes (scale bar, 1 nm). (**J**) Corresponding ratios of regenerated complex bonds from three stretching-releasing cycles of CG-MD results. (**K**) Comparison of the mechanical properties of the COMBIA hydrogel and other reported hydrogels reinforced by different strategies, such as dual cross-linked (DC), interpenetrating network (IPN), nanocomposite (NC), double network (DN), and metal ion cross-linked (MC) methods. The detailed data are summarized in table S2. (**L**) Mechanical properties of COMBIA compared to those of other metal ion cross-linked hydrogels reported in the literature (*35–38*).

more dominant at larger strains in the COMBIA hydrogel. These excellent performances were well maintained even at −20°C (Fig. 2D and fig. S6). Two key factors were identified for the substantially increased mechanical properties of the COMBIA hydrogel: cross-linked density and effective energy dissipation at the molecular scale. For our hydrogel with the COMBIA structure, the high cross-linking density via metal-ligand coordination interactions facilitated elastic deformation or ductility at large strains by increasing the bismuth ion concentration (Fig. 2C). Both the FTIR spectra and DFT calculations revealed the formation of hierarchical multiple reversible noncovalent bonds within the supramolecular network (Fig. 1, F and G), which contributed to the sufficient and reversible dissipation of energy when subjected to an external force (fig. S7). Moreover, the COMBIA hydrogel demonstrated high resilience (92.36% recovery at 100% strain), which is comparable to that of well-known highly resilient materials, including resilin in dragonfly tendons (92 to 97%), elastin in human skin and arteries (~90%), and polybutadiene rubber (80%) (Fig. 2E and fig. S8) (*34*). This is attributed to the spontaneous dissociation-reformation of hierarchical reversible noncovalent interactions during the extension-contraction of the COMBIA molecular network associated with chain straightening and alignment (fig. S9).

The structural evolution of our robust and mechanically resilient COMBIA hydrogels (Fig. 2, G to K; figs. S10 to S17; and Supplementary Texts 3 and 4) was investigated at the molecular level via coarse-grained molecular dynamics (CG-MD) simulations. As illustrated in Fig. 2F and fig. S12, COMBIA exhibited substantially enhanced performance compared to the control model and demonstrated qualitative alignment with the experimental results presented in Fig. 2C. Specifically, the polymer chain extension and sliding when stretched to 800% accounted for the ultraelastic characteristics of the COMBIA hydrogel (Fig. 2G and movie S2). Consequently, the polymer chain alignment was substantially improved, as evidenced by the increase in Herman's orientation factor (H_{of}) from 0.0397 for $\lambda = 2$, whereas the value of H_{of} was 0.1673 for $\lambda = 9$ (Fig. 2H). It was also observed that, during stretching, the density distributions of the bismuth-based complexes at different strains were negligible (Fig. 2I). This phenomenon is attributed to the dynamic behavior of the bismuth coordination bond, where dissociation-reformation events predominate during stretching. For instance, nearly 60% of the bismuth coordination bonds are regenerated when the sample is stretched to 200%, and this percentage increases further for subsequent stretching-releasing cycles (Fig. 2J). These results surpassed most of the previous results (Fig. 2K and table S2). For further comparative purposes, the comprehensive mechanical properties of hydrogels cross-linked with metal ions previously reported in the literature (*35*–*38*) are summarized in Fig. 2L and table S3. These findings suggest that the hierarchical multiple reversible physical interactions within the COMBIA structure could unify the different mechanical properties, introducing a powerful toolbox for fabricating a versatile platform.

Electrical, antifreezing, and self-healing properties of COMBIA hydrogels

The COMBIA hydrogels exhibited a conductivity as high as 7.52 S/m (Fig. 3A). This phenomenon is attributed to the synergistic effect of metal bismuth ions and an ion migration channel provided by the zwitterionic segments of the polymer chain (Fig. 3B). As demonstrated in Fig. 3 (C and D) and movie S3, the COMBIA hydrogel functioned as a conductor (even under stretching) in a circuit to illuminate a light-emitting diode (LED). Notably, the high conductivity, mechanical flexibility, and optical transparency of the COMBIA hydrogels were well maintained even at −20°C (Fig. 3A and fig. S18). This property is attributed to the low freezing point of the COMBIA hydrogel (−32.27°C) (fig. S19). In addition, superior moisturizing properties were observed for the hydrogel (fig. S20). Subsequently, the mechanical and electrical self-healing properties of the COMBIA hydrogel were examined. A key characteristic of physically cross-linked hydrogels is that the soft matrix is cross-linked by dynamic and reversible noncovalent interactions, generally enabling rapid self-healing with high efficiency (up to 100%). This characteristic resulted in mechanical self-healing, as evidenced by comparing the stress-strain characteristics of the original and damaged hydrogels after healing for various durations. The fracture toughness of the original (ε_{t0}) and healed (ε_t) hydrogels was used to evaluate the mechanical self-healing efficiency [δ_{MH}, which was calculated as $(\varepsilon_t / \varepsilon_{t0}) \times 100\%$]. The mechanical self-healing property is inherent to the zwitterionic network and is accomplished through the reformation of electrostatic interactions and hydrogen bonds (*39*). As presented in Fig. 3 (E to G), the COMBIA hydrogel demonstrated autonomous recovery from physical damage (Fig. 3E), and its healing efficiency reached 91.45% after leaving the cut-then-joint hydrogel for 250 min, which closely approximated the initial mechanical properties (Fig. 3, F and G). This ability is attributed to the rearrangement of entangled polymer chains to rebuild hierarchical dynamic interactions. Furthermore, the electrical self-healing efficiency [ϑ_{CH}, given as $\vartheta_{\text{CH}} = (\rho_c / \rho_{c0}) \times 100\%$] of the COMBIA hydrogel approached 100% (Fig. 3H and fig. S21). Note that ρ_{c0} represents the electrical conductivity before cutting, whereas ρ_c represents the electrical conductivity after self-healing. This is due to the instantaneous rebuilding of the ion transport channels. Crucially, analogous to human skin, the self-healing capability of our COMBIA hydrogel was repeatable (Fig. 3I), which is advantageous for long-term operation in practical applications. As a proof of concept, a battery-powered circuit was constructed, which further demonstrated the potential of electromechanical self-healing for electronic circuits (Fig. 3J and movies S4 and S5). It is worth noting that the substantially faster electrical healing compared to mechanical recovery is rooted in the distinct mechanisms governing these processes. Although electrical healing occurs almost instantaneously through rapid ionic rearrangement and transport, mechanical healing is inherently slower due to the time-dependent reentanglement of polymer chains and reestablishment of noncovalent interactions (i.e., hydrogen bonding, electrostatic interactions, and metal-ligand coordination). These molecular diffusion and chain realignment processes are influenced by polymer mobility, network density, and environmental factors (i.e., humidity and temperature). Consequently, mechanical recovery requires an extended timescale compared to the nearly instantaneous electrical restoration (*40*–*42*).

Self-adhesive properties of COMBIA hydrogels

The COMBIA hydrogel demonstrated the ability to adhere conformably to a human finger, even under joint movement (Fig. 4A and fig. S22). Notably, it exhibited reversible and strong adhesion to various hydrophobic and hydrophilic surfaces, such as glass, wood, poly(ethylene terephthalate) (PET), nylon, polyester, poly(methyl methacrylate) (PMMA), carbon fiber, and polyvinyl chloride (PVC) surfaces (Fig. 4B and movie S6). Through lap shear and 90° peeling experiments (Fig. 4, C to E), the high shear strength of the COMBIA hydrogel to various substrates was confirmed, ranging from 5.2 to 44.7 kPa. Furthermore, the adhesion strength of the COMBIA hydrogel was enhanced through in situ formation (fig. S23). For instance, the value formed in situ for glass materials increased to ~77.6 kPa from 44.7 kPa owing to the aggregation of abundant adhesive groups at the interface. Notably, this excellent self-adhesiveness was maintained even after long-term storage, 40 cycles of peeling/adhering, and washing with water (Fig. 4F and fig. S24). In addition, unlike the commercial VHB film, which lost its ability to adhere to water, the COMBIA hydrogel exhibited impressive underwater adhesion (fig. S25 and movie S7). The failure of VHB tape under underwater conditions could be attributed to the formation of an interfacial water

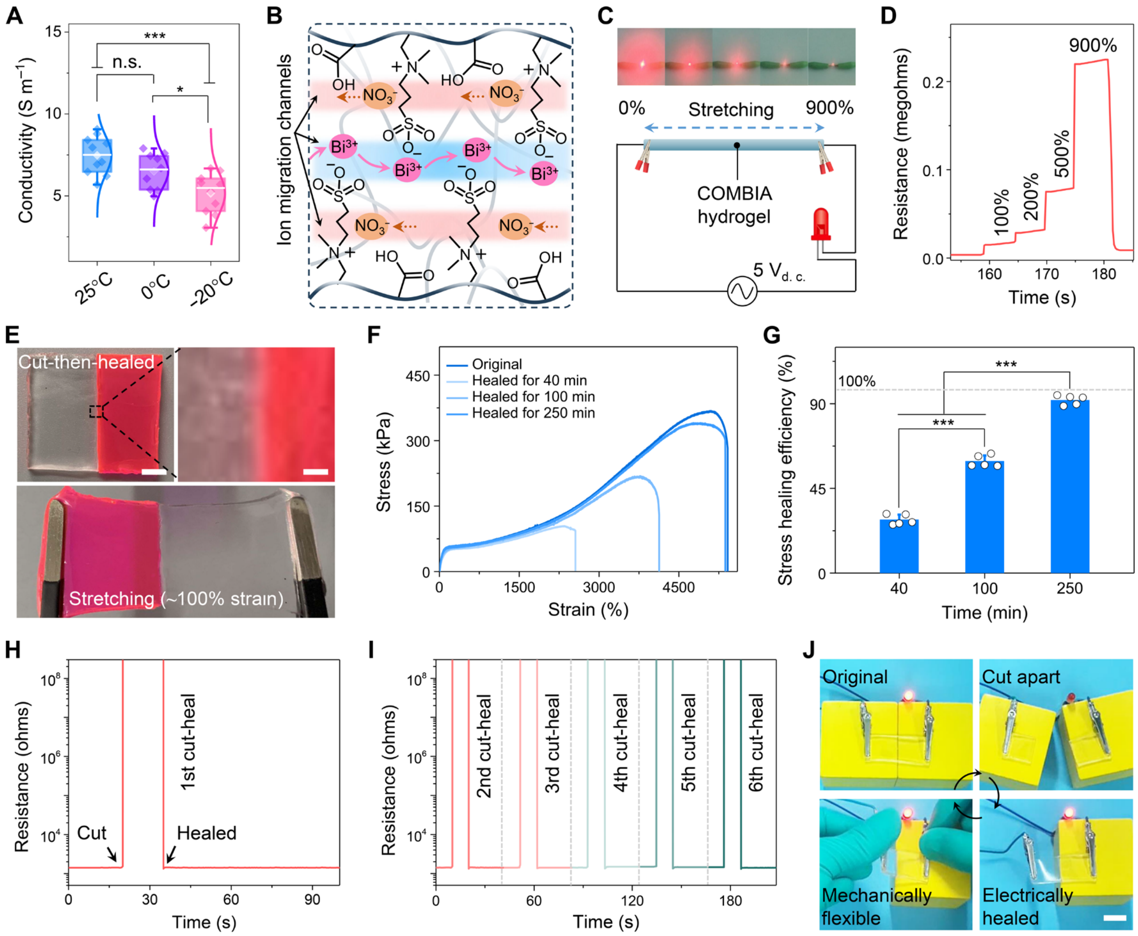

Fig. 3. Electrical, antifreezing, and self-healing properties of the COMBIA hydrogels. (**A**) Conductivity of COMBIA hydrogels at different temperatures. (**B**) Schematic illustration of the ion migration channels of COMBIA hydrogels. (**C**) LED brightness changes with increasing elongation of the COMBIA hydrogels. (**D**) Resistance changes of a hydrogel film conductor under axial stretching. (**E**) Macroscopic self-healing processes of the COMBIA hydrogel and then the stretching behaviors of the cut-then-healed hydrogel (top left: scale bar, 1 cm; top right: scale bar, 50 μm). (**F** and **G**) Stress-strain tests of initial and cut-then-healed COMBIA hydrogels at different healing times (F) and the corresponding stress self-healing efficiency (G). The error bars indicate the SD, $*P < 0.05$; $***P < 0.001$; n.s. (not significant) $P > 0.05$. (**H**) Resistance changes occurring during the cutting-healing procedures. (**I**) Repeated electrical self-healing ability of the COMBIA hydrogel. (**J**) Demonstration of the electrical healing process for a COMBIA hydrogel using a red LED indicator (scale bar, 1 cm; movie S4).

film and the lack of strong chemical interactions, which impeded adhesion in wet conditions. In contrast, the COMBIA hydrogel effectively overcame these limitations by its high deformability and adaptability, as well as the formation of dynamic noncovalent interactions with the substrate, including hydrogen bonding, electrostatic attractions, and metal-ligand coordination. These interactions effectively displaced interfacial water and facilitated strong adhesion, making the COMBIA hydrogel highly suitable for wet/underwater environments (*43*–*47*). Figure 4G presents a comparison of the shear strength between the results of the COMBIA hydrogels and those of previous studies, revealing the advantages of our strategy. The high shear strength can be attributed to the diverse chemical bonds within the adhesive interfaces, including hydrogen bonds, cation-π interactions, ion-dipole interactions, and electrostatic attractions (*47*–*54*), as shown in Fig. 4H and fig. S26. These hierarchical multiple reversible noncovalent interactions also confer upon the hydrogel a remarkable ability to resist interfacial cracking.

Multimodal self-powered sensing of the COMBIA e-skins

Given the optimal combination of multiple functions, including outstanding mechanical and electrical properties, the sensory capacities of the skin-like COMBIA hydrogel to external stimuli (i.e., strain, vibration, pressure, and temperature) were investigated. First, the sensitivity of COMBIA (fig. S27) increased considerably from 3.76 at 0 to 500% strain, 15.81 at 500 to 1600% strain, 57.74 at 1600 to 3100% strain, to 197.68 at 3100 to 5300% strain (Fig. 5A). Notably, the sensitivity of COMBIA at high strains exceeded that of all previously reported hydrogel sensors (Fig. 5B and table S4). Second, the sensing performance remained consistent across the applied strain rates from 25 to 250 mm min^{-1} under the same strain (150%; Fig. 5C), confirming the structural stability of COMBIA. Third, a sensing response time (137-ms response time and 162-ms recovery time) and a stable sensing signal at both small (0 to 6%) and large strains (20 to 300%) were achieved (Fig. 5D and fig. S28). Furthermore, the sensing stability was demonstrated by the negligible signal change

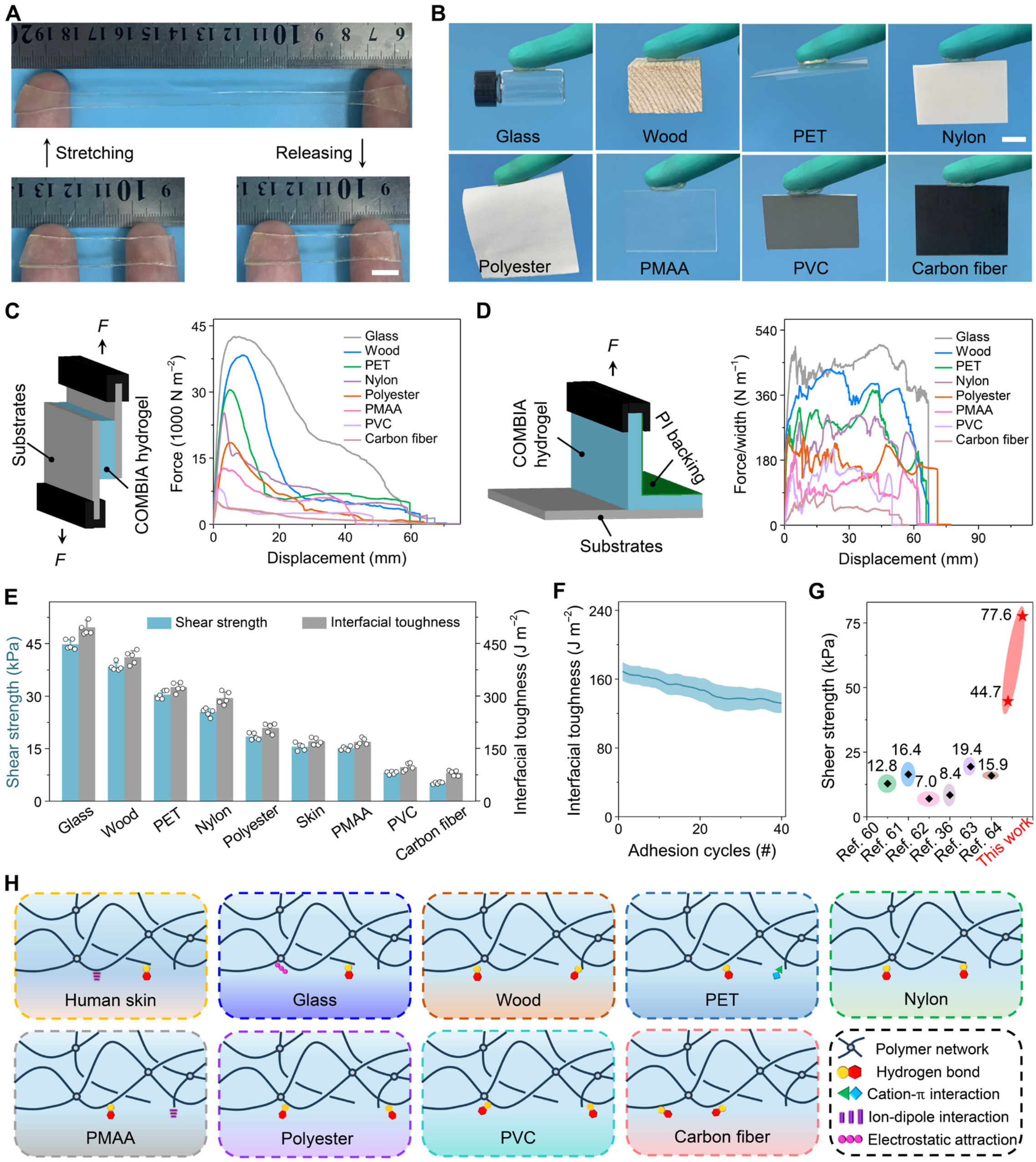

Fig. 4. Self-adhesive properties of the COMBIA hydrogels. (**A**) COMBIA hydrogel film exhibited direct adhesion to fingers and demonstrated resistance to stretching (scale bar, 1 cm). (**B**) Photos of COMBIA hydrogels adhered to glass, wood, PET, nylon, polyester, PMAA, carbon fiber, and PVC (scale bar, 1 cm). (**C** and **D**) Representative curves of the lapping (C) and peeling (D) strength of the COMBIA hydrogel on different solid substrates. (**E**) Shear strength and interfacial toughness. The error bars indicate the SD, $n = 5$ independent measurements. (**F**) Repeated adhesion to porcine skin through cycling in the adhering-stripping test. (**G**) Adhesive strengths of our COMBIA in adhering glass compared with other values reported in the literature (*36*, *60–64*). (**H**) Proposed adhesion mechanism between the COMBIA hydrogels and various substrates.

over 6500 loading-unloading cycles, as shown in Fig. 5F. Excellent sensing performance was maintained even at −20°C (Fig. 5E) or after the samples were cut and subsequently healed (fig. S29). For comparative purposes, previous hydrogel sensors were comprehensively reviewed and are summarized in Fig. 5L, fig. S30, and table S4. The COMBIA sensor demonstrates superior performance compared to most existing sensors, particularly in terms of combined sensing features and multiple functions. For instance, a COMBIA hydrogel as an e-skin can be readily attached to the epidermal system, including the finger, elbow, and face, to monitor movement and temperature (Fig. 5, G to J, and fig. S31). In addition, different hand gestures can be recognized when the COMBIA sensor array is used (Fig. 5K), indicating its potential in wearable devices.

A self-powered COMBIA e-skin was developed using triboelectric technology in the single-electrode mode (fig. S32). The COMBIA film devices exhibited high transparency (96.05%) as well

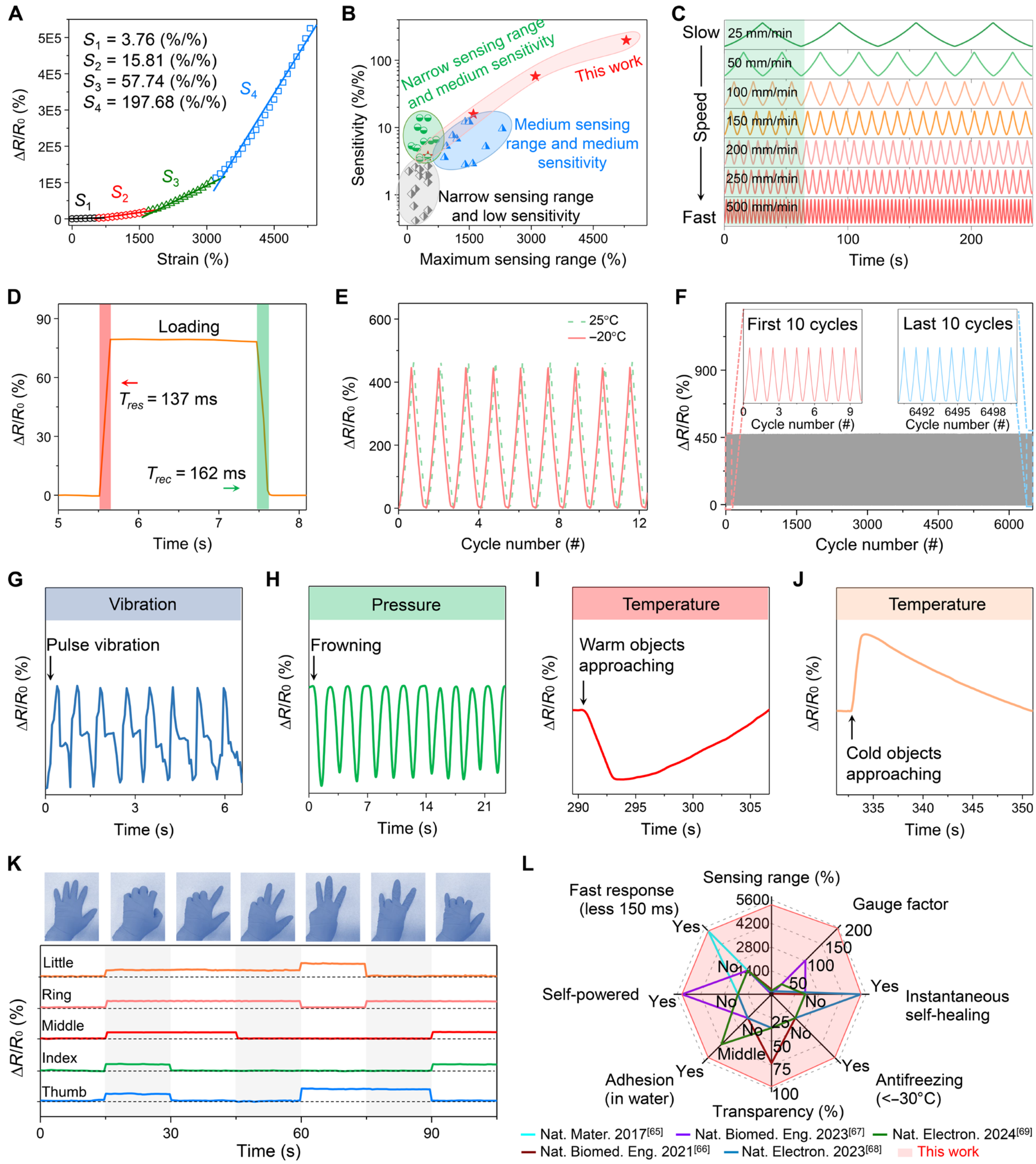

Fig. 5. Sensing performances of the COMBIA hydrogel e-skins. (**A**) Relative resistance variation ($\Delta R/R_0$) and sensitivity of COMBIA hydrogels at different strains. (**B**) Working range and sensitivity of this work compared with those reported in the literature in recent years. (**C**) Sensing signals under cyclic stretching-releasing at different motion speeds from 25 to 500 mm/min. (**D**) Response and recovery time of the COMBIA hydrogels to strain. (**E**) Sensing signals at subzero temperatures. (**F**) Sensing stability after more than 6500 loading-unloading cycles at 150% strain. (**G** to **J**) Multiple monitoring methods using a hydrogel film sensor, including pulse vibration (G), pressure (H), warming (I), and cooling (J). (**K**) Multichannel monitoring of gestures with five adhered COMBIA hydrogel e-skin sensors. (**L**) Comprehensive properties of COMBIA hydrogel film sensors compared to those of other soft electronics reported in the literature (*65–69*).

as excellent stretchability and softness (figs. S1 and S33). With dimensions of 33 mm by 38 mm, the electric output of the film device showed a typical open-circuit voltage (V_{OC}) of 233 V, short-circuit current (I_{SC}) of 14.6 μA, and short-circuit charge (Q_{SC}) of 127 nC (fig. S34A). The maximum output power density was calculated to be 1.71 W/m^2 with a load resistance of 10 megohms (fig. S34B). This energy output capability is sufficient for charging capacitors to power commercial electronics (figs. S35 and S36 and movie S8). Furthermore, a high electrical output was maintained even under high stretching conditions (fig. S37), in cut-then-healed states (fig. S38), and in low-temperature scenarios (fig. S39). The robustness of the film devices was further validated by repeatedly tapping the device for over 15,000 contact-separation cycles (fig. S40). The durability of the COMBIA film devices ensured their stable performance when applied for the detection of human movement (fig. S41). In comparison to previous reports, our COMBIA film device simultaneously integrated multiple functions that have rarely been reported before (fig. S42 and table S5). As detailed in figs. S43 and S44 and tables S3 and S6, none of the previously reported hydrogels exhibited the aforementioned all-in-one properties.

DISCUSSION

This study demonstrated a human skin-like multifunctional hydrogel via a facile manipulation process by creating a bismuth ion–coordinated polymer framework with a zwitterionic supramolecular network. Hierarchical, multiple reversible noncovalent interactions, such as bismuth-based coordinations, hydrogen bonds, and electrostatic attractions within the supramolecular network, endowed the COMBIA hydrogel with an unparalleled combination of functional merits. This unique combination, analogous to biological skin, is challenging to achieve in its artificial analogs, including being highly stretchable (5417% strain), highly mechanically rigid (12.14 MJ m^{-3}), skin-analogously soft (128.3-kPa Young's modulus), viscoelastic, sufficiently self-adhesive (44.7 kPa), repeatedly electrically and mechanically self-healing, and superiorly multimodal sensing. Notably, the bismuth ions in the COMBIA hydrogel matrix not only enabled the construction of a desirable homogeneous network microstructure, leading to high conductivity (7.52 S m^{-1}) and remarkable optical transparency (97.46%), but also synergized with glycerol, enabling the hydrogel to obtain high freeze tolerance (−32.27°C). A strain-sensing sensitivity of 197.68 and an excellent output power density of 1.71 W/m^2 were simultaneously achieved for the self-powered COMBIA e-skin. Considering the optimized combination of optical transparency, adhesion, and ambient stability, the COMBIA e-skin exhibits excellent potential as a highly sensitive and durable sensor for application in human-machine interfaces, intelligent robots, wearable devices, etc. It is anticipated that the proposed concept may offer a potential versatile platform that can be readily extended to prepare other soft conductive materials with a set of functional combinations.

MATERIALS AND METHODS

Materials

MH, bismuth nitrate pentahydrate [$Bi(NO_3)_3{\cdot}5H_2O$], 2-hydroxy-4′-(2-hydroxyethoxy)-2-methylpropiophenone (HP), and glycerol were supplied by Aladdin Chemistry Co. AA and poly(dimethylsiloxane) (PDMS) films were obtained from Tianjin Damao Chemical Reagent Co. and Hangzhou Bald Advanced Materials Co., respectively. Dielectric elastomer Very High Bond (VHB) 4905/4910 was obtained from 3M Co. Ultrapure water was used throughout the experiment.

Synthesis of freestanding COMBIA hydrogels

The COMBIA conductive hydrogel was synthesized as follows: Initially, various $Bi(NO_3)_3{\cdot}5H_2O$ solutions were dissolved in a glycerol/water cosolvent to form a homogeneous solution under vigorous stirring for 15 min, and a glycerol/water binary solvent was selected as the dispersion medium. In this study, the weight ratio, γ, of $Bi(NO_3)_3{\cdot}5H_2O$:MH/AA was adjusted from 0.2 to 0.8, and the control sample was poly(MH-AA) hydrogel (γ = 0, namely, PMA). Subsequently, AA (2.53 g) and MH (1.52 g) were added to the corresponding mixed solvent mentioned above and stirred for 25 min, after which the base concentration compared with that of the glycerol/water cosolvent was fixed. The photoinitiator HP (0.0135 g) was then added to the reaction system, followed by stirring for another 30 min. Notably, all hydrogel fabrication processes were conducted inside a glove box filled with nitrogen. To obtain freestanding COMBIA hydrogel films, the aforementioned solution was blown with argon in an argon atmosphere to remove dissolved oxygen. Subsequently, the solution was added to a custom-made PMMA mold for photocuring under ultraviolet (UV) light (365 nm, 35 W).

Self-powered COMBIA hydrogel e-skin

As a sensing material, the COMBIA hydrogels were cut into segments of desired lengths without any posttreatment for the fabrication of e-skins (fig. S27). Owing to their excellent tissue adhesiveness, they could be directly adhered to the human epidermis, thereby enabling sensitive wearable electronics. In this study, the sensitivity of COMBIA-based e-skins was defined as the slope of the relative resistance variation $[(R - R_0)/R_0]$ versus the strain curve, and human motions, including finger bending, elbow flexion, cheek bulging, and smiling, were also monitored by sensitive sensors. The resistance changes of the film sensors during human motion were recorded using a multimeter (model 34461A Keysight). For self-powered sensing devices, a COMBIA film as the electrode was encapsulated with PDMS layers, and its detailed structure is shown in fig. S32.

Characterization

A Nicolet IS50 attenuated total reflectance–FTR instrument (Thermo Fisher Scientific, USA) and XPS (Escalab 250Xi, Thermo Fisher Scientific Co., USA) were used to investigate the chemical structure of the hydrogel samples. A Zeiss Supra 55 field-emission scanning electron microscope (Carl Zeiss AG, Germany) was used to examine the surface morphologies of the freeze-dried as-prepared hydrogels. Differential scanning calorimetry (DSC 4000, PerkinElmer Co., USA) was used to study the antifreezing properties of the as-prepared hydrogels. A Lambda-950 UV-visible spectrometer (PerkinElmer Co., USA) was used to characterize the optical transmittance of the samples in the visible light wavelength range (380 to 780 nm). A WDW3100 mechanical tester (Changchun Kexin Co., China) was used to test the tensile properties of the hydrogel samples. The samples were secured between the two clamps, with the top clamp applying a uniaxial stretching force. It is worth noting that tensile tests were conducted following the ASTM D412 standard to evaluate the mechanical properties of the COMBIA hydrogel (*55–59*). Dog bone–shaped specimens with an overall length of 115 mm, a gauge length of 25 mm, a narrow section width of 6 mm, and a thickness of 2 mm were used. The tests were performed under controlled environmental conditions of 25°C and 80% relative humidity to ensure consistency and reproducibility. The conductivity was derived from electrochemical impedance spectroscopy data measured by an electrochemical workstation (CHI660E, CH Instruments Inc.). Optical images were captured using a Digital Single Lens Reflex (Canon EOS 200D2). When subjected to various strains, the resistance changes ($\Delta R/R_0$) of the hydrogel films were recorded using a multimeter (model 34461A Keysight). The electric output performances, including V_{OC}, I_{SC}, and Q_{SC}, of the self-powered COMBIA hydrogel film were investigated using a Keithley 6514 programmable electrometer. Informed consent was obtained from all participants, and the study adhered to all relevant ethical regulations.

Supplementary Materials

The PDF file includes:
Supplementary Texts 1 to 4
Figs. S1 to S44
Tables S1 to S6
Legends for movies S1 to S8
References

Other Supplementary Material for this manuscript includes the following:
Movies S1 to S8

REFERENCES AND NOTES

1. W. Wang, Y. Jiang, D. Zhong, Z. Zhang, S. Choudhury, J.-C. Lai, H. Gong, S. Niu, X. Yan, Y. Zheng, C.-C. Shih, R. Ning, Q. Lin, D. Li, Y.-H. Kim, J. Kim, Y.-X. Wang, C. Zhao, C. Xu, X. Ji, Y. Nishio, H. Lyu, J. B.-H. Tok, Z. Bao, Neuromorphic sensorimotor loop embodied by monolithically integrated, low-voltage, soft e-skin. *Science* **380**, 735–742 (2023).
2. Z. Liu, X. Hu, R. Bo, Y. Yang, X. Cheng, W. Pang, Q. Liu, Y. Wang, S. Wang, S. Xu, Z. Shen, Y. Zhang, A three-dimensionally architected electronic skin mimicking human mechanosensation. *Science* **384**, 987–994 (2024).
3. C. Xu, Y. Song, J. R. Sempionatto, S. A. Solomon, Y. Yu, H. Y. Y. Nyein, R. Y. Tay, J. Li, W. Heng, J. Min, A. Lao, T. K. Hsiai, J. A. Sumner, W. Gao, A physicochemical-sensing electronic skin for stress response monitoring. *Nat. Electron.* **7**, 168–179 (2024).
4. F. Liu, S. Deswal, A. Christou, Y. Sandamirskaya, M. Kaboli, R. Dahiya, Neuro-inspired electronic skin for robots. *Sci. Robot.* **7**, eabl7344 (2022).
5. J. Yi, G. Zou, J. Huang, X. Ren, Q. Tian, Q. Yu, P. Wang, Y. Yuan, W. Tang, C. Wang, L. Liang, Z. Cao, Y. Li, M. Yu, Y. Jiang, F. Zhang, X. Yang, W. Li, X. Wang, Y. Luo, X. J. Loh, G. Li, B. Hu, Z. Liu, H. Gao, X. Chen, Water-responsive supercontractile polymer films for bioelectronic interfaces. *Nature* **624**, 295–302 (2023).
6. H. Park, S. Kim, J. Lee, I. Lee, S. Bontapalle, Y. Na, K. Sim, Organic flexible electronics with closed-loop recycling for sustainable wearable technology. *Nat. Electron.* **7**, 39–50 (2024).
7. C.-C. Kim, H.-H. Lee, K. H. Oh, J.-Y. Sun, Highly stretchable, transparent ionic touch panel. *Science* **353**, 682–687 (2016).
8. M. Lin, H. Hu, S. Zhou, S. Xu, Soft wearable devices for deep-tissue sensing. *Nat. Rev. Mater.* **7**, 850–869 (2022).
9. C. Larson, B. Peele, S. Li, S. Robinson, M. Totaro, L. Beccai, B. Mazzolai, R. Shepherd, Highly stretchable electroluminescent skin for optical signaling and tactile sensing. *Science* **351**, 1071–1074 (2016).
10. B. C. K. Tee, J. Ouyang, Soft electronically functional polymeric composite materials for a flexible and stretchable digital future. *Adv. Mater.* **30**, e1802560 (2018).
11. L. Chen, Z. Jin, W. Feng, L. Sun, H. Xu, C. Wang, A hyperelastic hydrogel with an ultralarge reversible biaxial strain. *Science* **383**, 1455–1461 (2024).
12. X. Guo, F. Yang, X. Sun, C. Han, Y. Bai, G. Liu, W. Liu, R. Wang, Fabrication of a novel separation-free heterostructured photocatalyst with enhanced visible light activity in photocatalytic degradation of antibiotics. *J. Mater. Chem. A* **10**, 3146–3158 (2022).
13. S. Guo, S. Zhang, H. Li, S. Liu, J. J. Koh, M. Zhou, Z. Sun, Y. Liu, H. Qu, Z. Yu, Y. Zhang, L. Yang, W. Chen, C. He, C. Lee, D. Mao, S. K. Ravi, Y. Lai, S. C. Tan, Precisely manipulating polymer chain interactions for multifunctional hydrogels. *Matter* **7**, 1–17 (2024).
14. Y. Tian, Z. Wang, S. Cao, D. Liu, Y. Zhang, C. Chen, Z. Jiang, J. Ma, Y. Wang, Connective tissue inspired elastomer-based hydrogel for artificial skin via radiation-indued penetrating polymerization. *Nat. Commun.* **15**, 636 (2024).
15. G. Hou, X. Zhang, F. Du, Y. Wu, X. Zhang, Z. Lei, W. Lu, F. Zhang, G. Yang, H. Wang, Z. Liu, R. Wang, Q. Ge, J. Chen, G. Meng, N. X. Fang, X. Qian, Self-regulated underwater phototaxis of a photoresponsive hydrogel-based phototactic vehicle. *Nat. Nanotechnol.* **19**, 77–84 (2024).
16. H. Yuk, J. Wu, X. Zhao, Hydrogel interfaces for merging humans and machines. *Nat. Rev. Mater.* **7**, 935–952 (2022).
17. X. Guo, F. Yang, W. Liu, C. Han, Y. Bai, X. Sun, L. Hao, W. Jiao, R. Wang, Skin-inspired self-healing semiconductive touch panel based on novel transparent stretchable hydrogels. *J. Mater. Chem. A* **9**, 14806–14817 (2021).
18. Y. Wang, X. Huang, X. Zhang, Ultrarobust, tough and highly stretchable self-healing materials based on cartilage-inspired noncovalent assembly nanostructure. *Nat. Commun.* **12**, 1291 (2021).
19. G. Zhang, J. Steck, J. Kim, C. H. Ahn, Z. Suo, Hydrogels of arrested phase separation simultaneously achieve high strength and low hysteresis. *Sci. Adv.* **9**, eadh7742 (2023).
20. Y. S. Zhang, A. Khademhosseini, Advances in engineering hydrogels. *Science* **356**, eaaf3627 (2017).
21. J. Mintserisa, S. P. Gygi, High-density chemical cross-linking for modeling protein interactions. *Proc. Natl. Acad. Sci. U.S.A.* **117**, 93–102 (2020).
22. M. Preethi, C. Viswanathan, N. Ponpandian, A green path to extract carbon quantum dots by coconut water: Another fluorescent probe towards Fe^{3+} ions. *Particuology* **58**, 251–258 (2021).
23. Y. Liu, L. Zhang, L. Chen, Z. Liu, C. Liu, G. Che, 2-Hydroxynaphthalene based acylhydrazone as a turn-on fluorescent chemosensor for Al^{3+} detection and its real sample applications. *Spectrochim. Acta A Mol. Biomol. Spectrosc.* **248**, 119269 (2021).
24. R. Martin-Rodriguez, F. Aguado, M. D. Alba, R. Valiente, A. C. Perdigon, Eu^{3+} Luminescence in high charge mica: An in situ probe for the encapsulation of radioactive waste in geological repositories. *ACS Appl. Mater. Interfaces* **11**, 7559–7565 (2019).
25. S. Zhang, Y. Deng, A. Libanori, Y. Zhou, J. Yang, T. Tat, L. Yang, W. Sun, P. Zheng, Y.-L. Zhu, J. Chen, S. C. Tan, In situ grown silver-polymer framework with coordination complexes for functional artificial tissues. *Adv. Mater.* **35**, e2207916 (2023).
26. A. Imamura, M. Kimura, T. Kon, S. Sunohara, N. Kobayashi, Bi-based electrochromic cell with mediator for white/black imaging. *Sol. Energy Mater. Sol. Cells* **93**, 2079–2082 (2009).
27. Y. Mei, H. Xu, J. Zhang, Z. Ci, M. Duan, S. Peng, Z. Zhang, W. Tian, Y. Lu, Y. Wang, Design and spectral control of a novel ultraviolet emitting long lasting phosphor for assisting TiO_2 photocatalysis: Zn_2SiO_4:Ga^{3+}, Bi^{3+}. *J. Alloy. Compd.* **622**, 908–912 (2015).
28. I. M. El-Sewify, M. A. Shenashena, A. Shahatc, H. Yamaguchia, M. M. Selimd, M. M. H. Khalilb, S. A. El-Safty, Dual colorimetric and fluorometric monitoring of Bi^{3+} ions in water using supermicroporous Zr-MOFs chemosensors. *J. Lumin.* **198**, 438–448 (2018).
29. L. Tian, L. Wang, L. Zhang, Q. Zhang, W. Ding, M. Yu, Enhanced luminescence of Dy^{3+}/Bi^{3+} co-doped $Gd_3Al_5O_{12}$ phosphors by high-efficiency energy transfer. *J. Mater. Sci. Mater. Electron.* **26**, 8507–8514 (2015).
30. A. B. Asha, Y. Chen, R. Narain, Bioinspired dopamine and zwitterionic polymers for non-fouling surface engineering. *Chem. Soc. Rev.* **50**, 11668–11683 (2021).
31. Q. Shao, S. Jiang, Molecular understanding and design of zwitterionic materials. *Adv. Mater.* **27**, 15–26 (2015).
32. Q. Li, C. Wen, J. Yang, X. Zhou, Y. Zhu, J. Zheng, G. Cheng, J. Bai, T. Xu, J. Ji, S. Jiang, L. Zhang, P. Zhang, Zwitterionic biomaterials. *Chem. Rev.* **122**, 17073–17154 (2022).
33. Y. He, Q. Li, P. Chen, Q. Duan, J. Zhan, X. Cai, L. Wang, H. Hou, X. Qiu, A smart adhesive Janus hydrogel for non-invasive cardiac repair and tissue adhesion prevention. *Nat. Commun.* **13**, 7666 (2022).
34. X. Zhao, X. Chen, H. Yuk, S. Lin, X. Liu, G. Parada, Soft materials by design: Unconventional polymer networks give extreme properties. *Chem. Rev.* **121**, 4309–4372 (2021).
35. C.-W. Lai, S.-S. Yu, 3D printable strain sensors from deep eutectic solvents and cellulose nanocrystals. *ACS Appl. Mater. Interfaces* **12**, 34235–34244 (2020).
36. Z. He, Z. Zhou, W. Yuan, Highly adhesive, stretchable, and antifreezing hydrogel with excellent mechanical properties for sensitive motion sensors and temperature-/humidity-driven actuators. *ACS Appl. Mater. Interfaces* **14**, 38205–38215 (2022).
37. L. Chen, X. Chang, J. Chen, Y. Zhu, Ultrastretchable, antifreezing, and high-performance strain sensor based on a muscle-inspired anisotropic conductive hydrogel for human motion monitoring and wireless transmission. *ACS Appl. Mater. Interfaces* **14**, 43833–43843 (2022).
38. S. Guo, H.-Y. Chang, M.-J. Xu, C.-X. Wang, H. Wei, D.-D. Li, J. Chen, Y. Zhou, Y. Liu, Co^{2+}-mediated hydrogels with enhanced mechanical properties for flexible sensing. *ACS Appl. Polym. Mater.* **4**, 6403–6413 (2022).
39. R. Nasseri, N. Bouzari, J. Huang, H. Golzar, S. Jankhani, X. S. Tang, T. H. Mekonnen, A. Aghakhani, H. Shahsavan, Programmable nanocomposites of cellulose nanocrystals and zwitterionic hydrogels for soft robotics. *Nat. Commun.* **14**, 6108 (2023).
40. D. L. Taylor, M. i. h. Panhuis, Self-healing hydrogels. *Adv. Mater.* **28**, 9060–9093 (2016).
41. Y. Yanagisawa, Y. Nan, K. Okuro, T. Aida, Mechanically robust, readily repairable polymers via tailored noncovalent cross-linking. *Science* **359**, 72–76 (2018).
42. Y. Zhou, L. Li, Z. Han, Q. Li, J. He, Q. Wang, Self-healing polymers for electronics and energy devices. *Chem. Rev.* **123**, 558–612 (2023).
43. J. Yu, R. Xie, M. Zhang, K. Shen, Y. Yang, X. Zhao, X. Zhang, Y. Zhang, Y. Cheng, Molecular architecture regulation for the design of instant and robust underwater adhesives. *Sci. Adv.* **9**, eadg4031 (2023).
44. J. Wei, P. Xiao, T. Chen, Water-resistant conductive gels toward underwater wearable sensing. *Adv. Mater.* **35**, e2211758 (2023).
45. A. Narayanan, A. Dhinojwala, A. Joy, Design principles for creating synthetic underwater adhesives. *Chem. Soc. Rev.* **50**, 13321–13345 (2021).
46. A. H. Hofman, I. A. van Hees, J. Yang, M. Kamperman, Bioinspired underwater adhesives by using the supramolecular toolbox. *Adv. Mater.* **30**, e1704640 (2018).
47. H. Fan, J. P. Gong, Bioinspired underwater adhesives. *Adv. Mater.* **33**, e2102983 (2021).
48. G. Gao, F. Yang, F. Zhou, J. He, W. Lu, P. Xiao, H. Yan, C. Pan, T. Chen, Z. L. Wang, Bioinspired self-healing human-machine interactive touch pad with pressure-sensitive adhesiveness on targeted substrates. *Adv. Mater.* **32**, e2004290 (2020).
49. K. Shen, Z. Lv, Y. Yang, H. Wang, J. Liu, Q. Chen, Z. Liu, M. Zhang, J. Liu, Y. Cheng, A wet-adhesion and swelling-resistant hydrogel for fast hemostasis, accelerated tissue injury healing and bioelectronics. *Adv. Mater.* **37**, e2414092 (2024).
50. H. Fan, J. Wang, Z. Tao, J. Huang, P. Rao, T. Kurokawa, J. P. Gong, Adjacent cationic-aromatic sequences yield strong electrostatic adhesion of hydrogels in seawater. *Nat. Commun.* **10**, 5127 (2019).

51. X. Ma, X. Zhou, J. Ding, B. Huang, P. Wang, Y. Zhao, Q. Mu, S. Zhang, C. Ren, W. Xu, Hydrogels for underwater adhesion: Adhesion mechanism, design strategies and applications. *J. Mater. Chem. A* **10**, 11823–11853 (2022).
52. Y. Zhao, S. Song, X. Ren, J. Zhang, Q. Lin, Y. Zhao, Supramolecular adhesive hydrogels for tissue engineering applications. *Chem. Rev.* **122**, 5604–5640 (2022).
53. J. Yang, R. Bai, B. Chen, Z. Suo, Hydrogel adhesion: A supramolecular synergy of chemistry, topology, and mechanics. *Adv. Funct. Mater.* **30**, 1901693 (2019).
54. X. Guo, F. Yang, X. Sun, Y. Bai, G. Liu, W. Liu, R. Wang, X. He, Anti-freezing self-adhesive self-healing degradable touch panel with ultra-stretchable performance based on transparent triboelectric nanogenerators. *Adv. Funct. Mater.* **32**, 2201230 (2022).
55. H. Liu, D. Li, H. Chu, Y. Ding, Z. Fu, X. Yao, J. Zhu, J. Yang, R. Liu, T. Xu, S. Fu, Y. Liu, Y. Han, Y. Wang, Y. Zhao, X. Cui, Y. Tian, Ultra-stretchable triboelectric touch pad with sandpaper micro-surfaces for transformer-assisted gesture recognition. *Nano Energy* **130**, 110110 (2024).
56. H. Liu, Y. Li, Q. Sun, J. Yang, Y. Zhao, X. Cui, Y. Tian, Triboelectric wearable devices for accelerated wound healing. *Chem. Eng. J.* **497**, 154628 (2024).
57. Z. Fu, D. Li, H. Liu, R. Liu, Q. Lyu, Y. Han, Y. Wang, K. Zhang, G. Chen, Y. Tian, Antifreeze protein-based ultrastretchable and highly sensitive hydrogel for human-machine interaction. *Chem. Eng. J.* **488**, 150775 (2024).
58. J. Ma, S. Xing, Y. Wang, J. Yang, F. Yu, Kinetic-thermodynamic promotion engineering toward high-density hierarchical and Zn-doping activity-enhancing ZnNiO@CF for high-capacity desalination. *Nanomicro Lett.* **16**, 143 (2024).
59. R. Liu, Y. Liu, Y. Cheng, H. Liu, S. Fu, K. Jin, D. Li, Z. Fu, Y. Han, Y. Wang, Y. Tian, Aloe inspired special structure hydrogel pressure sensor for real-time human-computer interaction and muscle rehabilitation system. *Adv. Funct. Mater.* **33**, 2308175 (2023).
60. J. Yin, S. Pan, L. Wu, L. Tan, D. Chen, S. Huang, Y. Zhang, P. He, A self-adhesive wearable strain sensor based on a highly stretchable, tough, self-healing and ultra-sensitive ionic hydrogel. *J. Mater. Chem. C* **8**, 17349–17364 (2020).
61. Q. Ling, W. Liu, J. Liu, L. Zhao, Z. Ren, H. Gu, Highly sensitive and robust polysaccharide-based composite hydrogel sensor integrated with underwater repeatable self-adhesion and rapid self-healing for human motion detection. *ACS Appl. Mater. Interfaces* **14**, 24741–24754 (2022).
62. J. Liu, S. Bao, Q. Ling, X. Fan, H. Gu, Ultra-fast preparation of multifunctional conductive hydrogels with high mechanical strength, self-healing and self-adhesive properties based on Tara Tannin-Fe^{3+} dynamic redox system for strain sensors applications. *Polymer* **240**, 124513 (2022).
63. W. Zhang, Y. Zhang, Y. Dai, F. Xia, X. Zhang, Gradient adhesion modification of polyacrylamide/alginate-calcium tough hydrogels. *J. Mater. Chem. B* **10**, 757–764 (2022).
64. R. Liu, Y. Li, J. Chen, X. Zhang, Z. Niu, Y. Sun, The preparation of multifunction chitosan adhesive hydrogel by "one- step" method. *J. Biomater. Sci. Polym. Ed.* **31**, 1925–1940 (2020).
65. J. U. Lind, T. A. Busbee, A. D. Valentine, F. S. Pasqualini, H. Yuan, M. Yadid, S. J. Park, A. Kotikian, A. P. Nesmith, P. H. Campbell, J. J. Vlassak, J. A. Lewis, K. K. Parker, Instrumented cardiac microphysiological devices via multimaterial three-dimensional printing. *Nat. Mater.* **16**, 303–308 (2017).
66. J. Kim, J. Park, Y. G. Park, E. Cha, M. Ku, H. S. An, K. P. Lee, M. I. Huh, J. Kim, T. S. Kim, D. W. Kim, H. K. Kim, J. U. Park, A soft and transparent contact lens for the wireless quantitative monitoring of intraocular pressure. *Nat. Biomed. Eng.* **5**, 772–782 (2021).
67. K. Kwon, J. U. Kim, S. M. Won, J. Zhao, R. Avila, H. Wang, K. S. Chun, H. Jang, K. H. Lee, J. H. Kim, S. Yoo, Y. J. Kang, J. Kim, J. Lim, Y. Park, W. Lu, T. I. Kim, A. Banks, Y. Huang, J. A. Rogers, A battery-less wireless implant for the continuous monitoring of vascular pressure, flow rate and temperature. *Nat. Biomed. Eng.* **7**, 1215–1228 (2023).
68. Y. Zhao, Y. Ohm, J. Liao, Y. Luo, H.-Y. Cheng, P. Won, P. Roberts, M. R. Carneiro, M. F. Islam, J. H. Ahn, L. M. Walker, C. Majidi, A self-healing electrically conductive organogel composite. *Nat. Electron.* **6**, 206–215 (2023).
69. Y. Lu, G. Yang, S. Wang, Y. Zhang, Y. Jian, L. He, T. Yu, H. Luo, D. Kong, Y. Xianyu, B. Liang, T. Liu, X. Ouyang, J. Yu, X. Hu, H. Yang, Z. Gu, W. Huang, K. Xu, Stretchable graphene-hydrogel interfaces for wearable and implantable bioelectronics. *Nat. Electron.* **7**, 51–65 (2024).
70. C. Liu, F. Li, G. Li, P. Li, A. Hu, Z. Cui, Z. Cong, J. Niu, Zwitterionic hydrogel electrolyte with tunable mechanical and electrochemical properties for a wearable motion and thermal sensor. *ACS Appl. Mater. Interfaces* **14**, 9608–9617 (2022).
71. J. Song, Y. Zhu, J. Zhang, J. Yang, Y. Du, W. Zheng, C. Wen, Y. Zhang, L. Zhang, Encapsulation of AgNPs within zwitterionic hydrogels for highly efficient and antifouling catalysis in biological environments. *Langmuir* **35**, 1563–1570 (2019).
72. M. Kang, O. Oderinde, S. Liu, Q. Huang, W. Ma, F. Yao, G. Fu, Characterization of Xanthan gum-based hydrogel with Fe^{3+} ions coordination and its reversible sol-gel conversion. *Carbohydr. Polym.* **203**, 139–147 (2019).
73. S. Aleid, M. Wu, R. Li, W. Wang, C. Zhang, L. Zhang, P. Wang, Salting-in effect of zwitterionic polymer hydrogel facilitates atmospheric water harvesting. *ACS Mater. Lett.* **4**, 511–520 (2022).
74. F. Mo, Z. Chen, G. Liang, D. Wang, Y. Zhao, H. Li, B. Dong, C. Zhi, Zwitterionic sulfobetaine hydrogel electrolyte building separated positive/negative ion migration channels for aqueous Zn-MnO_2 batteries with superior rate capabilities. *Adv. Energy Mater.* **10**, 2000035 (2020).
75. S. J. Marrink, H. J. Risselada, S. Yefimov, D. P. Tieleman, A. H. de Vries, The MARTINI force field: Coarse grained model for biomolecular simulations. *J. Phys. Chem. B* **111**, 7812–7824 (2007).
76. Y. L. Zhu, H. Y. Zhao, C. L. Fu, Z. W. Li, Z. Y. Sun, Z. Lu, Mechanisms of defect correction by reversible chemistries in covalent organic frameworks. *J. Phys. Chem. Lett.* **11**, 9952–9956 (2020).
77. S. Zhang, Y. Zhou, A. Libanori, Y. Deng, M. Liu, M. Zhou, H. Qu, X. Zhao, P. Zheng, Y.-L. Zhu, J. Chen, S. C. Tan, Biomimetic spinning of soft functional fibres via spontaneous phase separation. *Nat. Electron.* **6**, 338–348 (2023).
78. H. Liu, Y. L. Zhu, Z. Y. Lu, F. Muller-Plathe, A kinetic chain growth algorithm in coarse-grained simulations. *J. Comput. Chem.* **37**, 2634–2646 (2016).
79. Y.-L. Zhu, D. Pan, Z.-W. Li, H. Liu, H.-J. Qian, Y. Zhao, Z.-Y. Lu, Z.-Y. Sun, Employing multi-GPU power for molecular dynamics simulation: An extension of GALAMOST. *Mol. Phys.* **116**, 1065–1077 (2018).
80. Y. L. Zhu, H. Liu, Z. W. Li, H. J. Qian, G. Milano, Z. Y. Lu, GALAMOST: GPU-accelerated large-scale molecular simulation toolkit. *J. Comput. Chem.* **34**, 2197–2211 (2013).
81. Y. Li, J. Yan, Y. Liu, X.-M. Xie, Super tough and intelligent multibond network physical hydrogels facilitated by $Ti_3C_2T_x$ MXene nanosheets. *ACS Nano* **16**, 1567–1577 (2022).
82. L. Zhou, Z. Wang, C. Wu, Y. Cong, R. Zhang, J. Fu, Highly sensitive pressure and strain sensors based on stretchable and recoverable ion-conductive physically cross-linked double-network hydrogels. *ACS Appl. Mater. Interfaces* **12**, 51969–51977 (2020).
83. S. Li, H. Pan, Y. Wang, J. Sun, Polyelectrolyte complex-based self-healing, fatigue-resistant and anti-freezing hydrogels as highly sensitive ionic skins. *J. Mater. Chem. A* **8**, 3667–3675 (2020).
84. H. Zhao, S. Hao, Q. Fu, X. Zhang, L. Meng, F. Xu, J. Yang, Ultrafast fabrication of lignin-encapsulated silica nanoparticles reinforced conductive hydrogels with high elasticity and self-adhesion for strain sensors. *Chem. Mater.* **34**, 5258–5272 (2022).
85. J. Zhang, Y. Gao, D. Liu, J. S. Zhao, J. Wang, Discharge domains regulation and dynamic processes of direct-current triboelectric nanogenerator. *Nat. Commun.* **14**, 3218 (2023).
86. Q. Fu, S. Hao, L. Meng, F. Xu, J. Yang, Engineering self-adhesive polyzwitterionic hydrogel electrolytes for flexible zinc-ion hybrid capacitors with superior low-temperature adaptability. *ACS Nano* **15**, 18469–18482 (2021).
87. X. Zhu, F. Guo, C. Ji, H. Mi, C. Liu, J. Qiu, Nitrogen-doped hollow carbon nanoboxes in zwitterionic polymer hydrogel electrolyte for superior quasi-solid-state zinc-ion hybrid supercapacitors. *J. Mater. Chem. A* **10**, 12856–12868 (2022).
88. J. Ren, Y. Liu, Z. Wang, S. Chen, Y. Ma, H. Wei, S. Lü, An anti-swellable hydrogel strain sensor for underwater motion detection. *Adv. Funct. Mater.* **32**, 2107404 (2021).
89. M. Yao, Z. Wei, J. Li, Z. Guo, Z. Yan, X. Sun, Q. Yu, X. Wu, C. Yu, F. Yao, S. Feng, H. Zhang, J. Li, Microgel reinforced zwitterionic hydrogel coating for blood-contacting biomedical devices. *Nat. Commun.* **13**, 5339 (2022).
90. K.-T. Huang, W.-H. Hung, Y.-C. Su, F.-C. Tang, L. D. Linh, C.-J. Huang, L.-H. Yeh, Zwitterionic gradient double-network hydrogel membranes with superior biofouling resistance for sustainable osmotic energy harvesting. *Adv. Funct. Mater.* **33**, 2211316 (2023).
91. J. Zhang, J. Zhuang, L. Lei, Y. Hou, Rapid preparation of a self-adhesive PAA ionic hydrogel using lignin sulfonate-Al^{3+} composite systems for flexible moisture-electric generators. *J. Mater. Chem. A* **11**, 3546–3555 (2023).
92. Y. Liang, J. Xue, B. Du, J. Nie, Ultrastiff, tough, and healable ionic-hydrogen bond cross-linked hydrogels and their uses as building blocks to construct complex hydrogel structures. *ACS Appl. Mater. Interfaces* **11**, 5441–5454 (2019).
93. H. Li, H. Zheng, Y. Tan, S. B. Tor, K. Zhou, Development of an ultrastretchable double-network hydrogel for flexible strain sensors. *ACS Appl. Mater. Interfaces* **13**, 12814–12823 (2021).
94. L. Fu, L. Li, Q. Bian, B. Xue, J. Jin, J. Li, Y. Cao, Q. Jiang, H. Li, Cartilage-like protein hydrogels engineered via entanglement. *Nature* **618**, 740–747 (2023).
95. S. Gantenbein, E. Colucci, J. Kach, E. Trachsel, F. B. Coulter, P. A. Ruhs, K. Masania, A. R. Studart, Three-dimensional printing of mycelium hydrogels into living complex materials. *Nat. Mater.* **22**, 128–134 (2023).
96. T. Zhou, H. Yuk, F. Hu, J. Wu, F. Tian, H. Roh, Z. Shen, G. Gu, J. Xu, B. Lu, X. Zhao, 3D printable high-performance conducting polymer hydrogel for all-hydrogel bioelectronic interfaces. *Nat. Mater.* **22**, 895–902 (2023).
97. B. R. Freedman, A. Kuttler, N. Beckmann, S. Nam, D. Kent, M. Schuleit, F. Ramazani, N. Accart, A. Rock, J. Li, M. Kurz, A. Fisch, T. Ullrich, M. W. Hast, Y. Tinguely, E. Weber, D. J. Mooney, Enhanced tendon healing by a tough hydrogel with an adhesive side and high drug-loading capacity. *Nat. Biomed. Eng.* **6**, 1167–1179 (2022).
98. M. Wang, Z. Yan, T. Wang, P. Cai, S. Gao, Y. Zeng, C. Wan, H. Wang, L. Pan, J. Yu, S. Pan, K. He, J. Lu, X. Chen, Gesture recognition using a bioinspired learning architecture that integrates visual data with somatosensory data from stretchable sensors. *Nat. Electron.* **3**, 563–570 (2020).

99. X. Ni, D. Liang, G. Zhou, C. Zhao, C. Chen, Bioinspired strategy to reinforce hydrogels via cooperative effect of dual physical cross-linkers. *Macromol. Chem. Phys.* **221**, 1900485 (2020).
100. M. Xia, S. Pan, H. Li, X. Yi, Y. Zhan, Z. Sun, X. Jiang, Y. Zhang, Hybrid double-network hydrogel for highly stretchable, excellent sensitive, stabilized, and transparent strain sensors. *J. Biomater. Sci. Polym. Ed.* **32**, 1548–1563 (2021).
101. Y.-Q. Wang, Y. Zhu, J.-H. Wang, X.-N. Li, X.-G. Wu, Y.-X. Qin, W.-Y. Chen, Fe^{3+}, NIR light and thermal responsive triple network composite hydrogel with multi-shape memory effect. *Compos. Sci. Technol.* **206**, 108653 (2021).
102. Y. Xin, J. Liang, L. Ren, W. Gao, W. Qiu, Z. Li, B. Qu, A. Peng, Z. Ye, J. Fu, G. Zeng, X. He, Tough, healable, and sensitive strain sensor based on multiphysically cross-linked hydrogel for ionic skin. *Biomacromolecules* **24**, 1287–1298 (2023).
103. Q. Zheng, L. Zhao, J. Wang, S. Wang, Y. Liu, X. Liu, High-strength and high-toughness sodium alginate/polyacrylamide double physically crosslinked network hydrogel with superior self-healing and self-recovery properties prepared by a one-pot method. *Colloids Surf. A Physicochem. Eng. Asp.* **589**, 124402 (2020).
104. J. Wen, M. Pan, J. Yuan, J. Wang, L. Zhu, Z. Jia, S. Song, Facile fabrication of dual-crosslinked single network heterostructural polyurethane hydrogels with superior mechanical and fluorescent performance. *React. Funct. Polym.* **146**, 104433 (2020).
105. B. Li, Y. Han, Y. Zhang, X. Cao, Z. Luo, Dual physically crosslinked nanocomposite hydrogels reinforced by poly(N-vinylpyrrolidone) grafted cellulose nanocrystal with high strength, toughness, and rapid self-recovery. *Cellulose* **27**, 9913–9925 (2020).
106. Z. Y. Chen, R. B. Zhou, R. D. Wang, S. L. Su, F. Zhou, Dual-crosslinked network of polyacrylamide-carboxymethylcellulose hydrogel promotes osteogenic differentiation in vitro. *Int. J. Biol. Macromol.* **234**, 123788 (2023).
107. Y. Wu, Y. Zeng, Y. Chen, C. Li, R. Qiu, W. Liu, Photocurable 3D printing of high toughness and self-healing hydrogels for customized wearable flexible sensors. *Adv. Funct. Mater.* **31**, 2107202 (2021).
108. J. Zheng, Y. Sun, S. Yang, Z. Li, X. Tang, X. Zeng, L. Lin, Cellulose nanocrystal reinforced conductive hydrogels with anti-freezing properties for strain sensors. *New J. Chem.* **46**, 20900–20908 (2022).
109. P. Huo, H. Ding, Z. Tang, X. Liang, J. Xu, M. Wang, R. Liang, G. Sun, Conductive silk fibroin hydrogel with semi-interpenetrating network with high toughness and fast self-recovery for strain sensors. *Int. J. Biol. Macromol.* **212**, 1–10 (2022).
110. F. Li, G. Zhang, Z. Wang, H. Jiang, S. Yan, L. Zhang, H. Li, Strong wet adhesion of tough transparent nanocomposite hydrogels for fast tunable focus lenses. *ACS Appl. Mater. Interfaces* **11**, 15071–15078 (2019).
111. H. Wang, J. Li, N. Ding, X. Zeng, X. Tang, Y. Sun, T. Lei, L. Lin, Eco-friendly polymer nanocomposite hydrogel enhanced by cellulose nanocrystal and graphitic-like carbon nitride nanosheet. *Chem. Eng. J.* **386**, 124021 (2020).
112. K. Xu, Y. Wang, B. Zhang, C. Zhang, T. Liu, Stretchable and self-healing polyvinyl alcohol/cellulose nanofiber nanocomposite hydrogels for strain sensors with high sensitivity and linearity. *Compos. Commun.* **24**, 100677 (2021).
113. K. Chen, Y. Hu, M. Liu, F. Wang, P. Liu, Y. Yu, Q. Feng, X. Xiao, Highly stretchable, tough, and conductive Ag@Cu nanocomposite hydrogels for flexible wearable sensors and bionic electronic skins. *Macromol. Mater. Eng.* **306**, 2100341 (2021).
114. F. Huang, W. Wei, Q. Fan, L. Li, M. Zhao, Z. Zhou, Super-stretchable and adhesive cellulose nanofiber-reinforced conductive nanocomposite hydrogel for wearable motion-monitoring sensor. *J. Colloid Interface Sci.* **615**, 215–226 (2022).
115. B. Li, Y. Chen, Y. Han, X. Cao, Z. Luo, Tough, highly resilient and conductive nanocomposite hydrogels reinforced with surface-grafted cellulose nanocrystals and reduced graphene oxide for flexible strain sensors. *Colloids Surf. A Physicochem. Eng. Asp.* **648**, 129341 (2022).
116. W. J. Han, J. H. Lee, J.-K. Lee, H. J. Choi, Remote-controllable, tough, ultrastretchable, and magneto-sensitive nanocomposite hydrogels with homogeneous nanoparticle dispersion as biomedical actuators, and their tuned structure, properties, and performances. *Compos. B Eng.* **236**, 109802 (2022).
117. W. Wang, Y. Chen, C. Xiao, S. Xiao, C. Wang, Q. Nie, P. Xu, J. Chen, R. You, G. Zhang, Y. Lu, Flexible SERS wearable sensor based on nanocomposite hydrogel for detection of metabolites and pH in sweat. *Chem. Eng. J.* **474**, 145953 (2023).
118. G. Chen, J. Huang, J. Gu, S. Peng, X. Xiang, K. Chen, X. Yang, L. Guan, X. Jiang, L. Hou, Highly tough supramolecular double network hydrogel electrolytes for an artificial flexible and low-temperature tolerant sensor. *J. Mater. Chem. A* **8**, 6776–6784 (2020).
119. J. Hua, C. Liu, P. F. Ng, B. Fei, Bacterial cellulose reinforced double-network hydrogels for shape memory strand. *Carbohydr. Polym.* **259**, 117737 (2021).
120. T. Wang, Y. Zhang, Z. Gu, W. Cheng, H. Lei, M. Qin, B. Xue, W. Wang, Y. Cao, Regulating mechanical properties of polymer-supramolecular double-network hydrogel by supramolecular self-assembling structures. *Chin. J. Chem.* **39**, 2711–2717 (2021).
121. R. Zeng, S. Lu, C. Qi, L. Jin, J. Xu, Z. Dong, C. Lei, Polyacrylamide/carboxymethyl chitosan double-network hydrogels with high conductivity and mechanical toughness for flexible sensors. *J. Appl. Polym. Sci.* **139**, 51993 (2021).
122. Z. Lei, W. Gao, P. Wu, Double-network thermocells with extraordinary toughness and boosted power density for continuous heat harvesting. *Joule* **5**, 2211–2222 (2021).
123. B. Zhou, Y. Li, Y. Chen, C. Gao, J. Li, Z. Bai, J. Guo, In situ synthesis of highly stretchable, freeze-tolerant silk-polyelectrolyte double-network hydrogels for multifunctional flexible sensing. *Chem. Eng. J.* **446**, 137405 (2022).
124. C. Du, J. Hu, X. Wu, H. Shi, H. C. Yu, J. Qian, J. Yin, C. Gao, Z. L. Wu, Q. Zheng, 3D printing of a tough double-network hydrogel and its use as a scaffold to construct a tissue-like hydrogel composite. *J. Mater. Chem. B* **10**, 468–476 (2022).
125. X. Zhang, H. Geng, X. Zhang, Y. Liu, J. Hao, J. Cui, Modulation of double-network hydrogels via seeding calcium carbonate microparticles for the engineering of ultrasensitive wearable sensors. *J. Mater. Chem. A* **11**, 2996–3007 (2023).
126. J. Zheng, G. Chen, H. Yang, C. Zhu, S. Li, W. Wang, J. Ren, Y. Cong, X. Xu, X. Wang, J. Fu, 3D printed microstructured ultra-sensitive pressure sensors based on microgel-reinforced double network hydrogels for biomechanical applications. *Mater. Horiz.* **10**, 4232–4242 (2023).
127. Y. Ren, J. Feng, Skin-inspired multifunctional luminescent hydrogel containing layered rare-earth hydroxide with 3D printability for human motion sensing. *ACS Appl. Mater. Interfaces* **12**, 6797–6805 (2020).
128. L. Liang, N. Sun, Y. Yu, S. Ren, A. Wu, L. Zheng, Photoluminescent polymer hydrogels with stimuli-responsiveness constructed from Eu-containing polyoxometalate and imidazolium zwitterions. *Soft Matter* **16**, 2311–2320 (2020).
129. Y. Yuan, H. Zhang, J. Qu, Pyridine-dicarbohydrazone-based polyacrylate hydrogels with strong mechanical property, tunable/force-induced fluorescence, and thermal/pH stimuli responsiveness. *ACS Appl. Polym. Mater.* **3**, 4512–4522 (2021).
130. Q. Zhu, L. Zhang, K. Van Vliet, A. Miserez, N. Holten-Andersen, White light-emitting multistimuli-responsive hydrogels with lanthanides and carbon dots. *ACS Appl. Mater. Interfaces* **10**, 10409–10418 (2018).
131. Y. Zhang, R. Wang, W. Lu, W. Li, S. Chen, T. Chen, Mechanical tough and multicolor aggregation-induced emissive polymeric hydrogels for fluorescent patterning. *Nanoscale Adv.* **5**, 725–732 (2023).
132. Z.-Y. Yuan, Z.-X. Cao, R. Wu, H. Li, Q.-J. Xu, H.-T. Wu, J. Zheng, J.-R. Wu, Ultra-robust metallosupramolecular hydrogels with unprecedented self-recoverability using asymmetrically distributed carboxyl-Fe^{3+} coordination interactions. *Chin. J. Polym. Sci.* **41**, 250–257 (2022).
133. T. Li, X. Hu, Q. Zhang, Y. Zhao, P. Wang, X. Wang, B. Qin, W. Lu, Poly(acrylic acid)-chitosan@tannic acid double-network self-healing hydrogel based on ionic coordination. *Polym. Adv. Technol.* **31**, 1648–1660 (2020).
134. Z. Jing, X. Xian, Q. Huang, Q. Chen, P. Hong, Y. Li, A. Shi, Biocompatible double network poly(acrylamide-co-acrylic acid)-Al^{3+}/poly(vinyl alcohol)/graphene oxide nanocomposite hydrogels with excellent mechanical properties, self-recovery and self-healing ability. *New J. Chem.* **44**, 10390–10403 (2020).
135. L. Zhang, J. Wang, J. Zhang, L. Hou, D. Ye, X. Jiang, Preparation of tough and anti-freezing hybrid double-network carboxymethyl chitosan/poly(acrylic amide) hydrogel and its application for flexible strain sensor. *J. Mater. Sci.* **57**, 19666–19680 (2022).
136. Z. Jing, Q. Zhang, Y. Q. Liang, Z. Zhang, P. Hong, Y. Li, Synthesis of poly(acrylic acid)-Fe^{3+}/gelatin/poly(vinyl alcohol) triple-network supramolecular hydrogels with high toughness, high strength and self-healing properties. *Polym. Int.* **68**, 1710–1721 (2019).
137. Q. Wang, X. Pan, C. Lin, X. Ma, S. Cao, Y. Ni, Ultrafast gelling using sulfonated lignin-Fe^{3+} chelates to produce dynamic crosslinked hydrogel/coating with charming stretchable, conductive, self-healing, and ultraviolet-blocking properties. *Chem. Eng. J.* **396**, 125341 (2020).
138. N. Li, D. Sun, Z. Su, X. Hao, M. Li, J. Ren, F. Peng, Rapid fabrication of xylan-based hydrogel by graft polymerization via a dynamic lignin-Fe^{3+} plant catechol system. *Carbohydr. Polym.* **269**, 118306 (2021).
139. Y. Wang, H. Zhang, H. Zhang, J. Chen, B. Li, S. Fu, Synergy coordination of cellulose-based dialdehyde and carboxyl with Fe^{3+} recoverable conductive self-healing hydrogel for sensor. *Mater. Sci. Eng. C* **125**, 112094 (2021).
140. Y. Chen, D. Wang, A. Mensaha, Q. Wang, Y. Cai, Q. Wei, Ultrafast gelation of multifunctional hydrogel/composite based on self-catalytic Fe^{3+}/Tannic acid-cellulose nanofibers. *J. Colloid Interface Sci.* **606**, 1457–1468 (2022).
141. J. Xu, Z. Wang, J. You, X. Li, M. Li, X. Wu, C. Li, Polymerization of moldable self-healing hydrogel with liquid metal nanodroplets for flexible strain-sensing devices. *Chem. Eng. J.* **392**, 123788 (2020).
142. J. Huang, M. Zhao, Y. Cai, M. Zimniewska, D. Li, Q. Wei, A dual-mode wearable sensor based on bacterial cellulose reinforced hydrogels for highly sensitive strain/pressure sensing. *Adv. Electron. Mater.* **6**, 1900934 (2019).
143. J. Chen, L. Zhang, Y. Tu, Q. Zhang, F. Peng, W. Zeng, M. Zhang, X. Tao, Wearable self-powered human motion sensors based on highly stretchable quasi-solid state hydrogel. *Nano Energy* **88**, 106272 (2021).
144. X. Sun, S. He, M. Yao, X. Wu, H. Zhang, F. Yao, J. Li, Fully-physically crosslinked silk fibroin/poly(hydroxyethyl acrylamide) hydrogel with high transparency and adhesive properties for wireless sensing and low-temperature strain sensing. *J. Mater. Chem. C* **9**, 1880–1887 (2021).
145. X. Liu, Z. Wu, D. Jiang, N. Guo, Y. Wang, T. Ding, L. Weng, A highly stretchable, sensing durability, transparent, and environmentally stable ion conducting hydrogel strain

sensor built by interpenetrating Ca^{2+}-SA and glycerol-PVA double physically cross-linked networks. *Adv. Compos. Hybrid Mater.* **5**, 1712–1729 (2022).
146. B. Zheng, H. Zhou, Z. Wang, Y. Gao, G. Zhao, H. Zhang, X. Jin, H. Liu, Z. Qin, W. Chen, A. Ma, W. Zhao, Y. Wu, Fishing net-inspired mutiscale ionic organohydrogels with outstanding mechanical robustness for flexible electronic devices. *Adv. Funct. Mater.* **33**, 2213501 (2023).
147. X. Jing, P. Feng, Z. Chen, Z. Xie, H. Li, X.-F. Peng, H.-Y. Mi, Y. Liu, Highly stretchable, self-healable, freezing-tolerant, and transparent polyacrylic acid/nanochitin composite hydrogel for self-powered multifunctional sensors. *ACS Sustain. Chem. Eng.* **9**, 9209–9220 (2021).
148. C. Luo, M. Huang, H. Liu, A highly resilient and ultra-sensitive hydrogel for wearable sensors. *J. Appl. Polym. Sci.* **139**, 51925 (2021).
149. L. Bai, Y. Jin, X. Shang, H. Jin, Y. Zhou, L. Shi, Highly synergistic, electromechanical and mechanochromic dual-sensing ionic skin with multiple monitoring, antibacterial, self-healing, and anti-freezing functions. *J. Mater. Chem. A* **9**, 23916–23928 (2021).
150. X. Zhang, C. Cui, S. Chen, L. Meng, H. Zhao, F. Xu, J. Yang, Adhesive ionohydrogels based on ionic liquid/water binary solvents with freezing tolerance for flexible ionotronic devices. *Chem. Mater.* **34**, 1065–1077 (2022).
151. P.-C. Lai, Z.-F. Ren, S.-S. Yu, Thermally induced gelation of cellulose nanocrystals in deep eutectic solvents for 3D printable and self-healable ionogels. *ACS Appl. Polym. Mater.* **4**, 9221–9230 (2022).
152. J. Xu, R. Jin, X. Ren, G. Gao, Cartilage-inspired hydrogel strain sensors with ultrahigh toughness, good self-recovery and stable anti-swelling properties. *J. Mater. Chem. A* **7**, 25441–25448 (2019).
153. F. Lu, Y. Wang, C. Wang, S. Kuga, Y. Huang, M. Wu, Two-dimensional nanocellulose-enhanced high-strength, self-adhesive, and strain-sensitive poly(acrylic acid) hydrogels fabricated by a radical-induced strategy for a skin sensor. *ACS Sustain. Chem. Eng.* **8**, 3427–3436 (2020).
154. H. Zhou, S. Li, H. Liu, B. Zheng, X. Jin, A. Ma, W. Chen, High-performance flexible sensors of self-healing, reversibly adhesive, and stretchable hydrogels for monitoring large and subtle strains. *Macromol. Mater. Eng.* **305**, 1900621 (2019).
155. J. Wang, Y. Liu, S. Wang, X. Liu, Y. Chen, P. Qi, X. Liu, Molybdenum disulfide enhanced polyacrylamide-acrylic acid-Fe^{3+} ionic conductive hydrogel with high mechanical properties and anti-fatigue abilities as strain sensors. *Colloids Surf. A Physicochem. Eng. Asp.* **610**, 125692 (2021).
156. X. Wei, D. Chen, X. Zhao, J. Luo, H. Wang, P. Jia, Underwater adhesive HPMC/SiW-PDMAEMA/Fe^{3+} hydrogel with self-healing, conductive, and reversible adhesive properties. *ACS Appl. Polym. Mater.* **3**, 837–846 (2021).
157. R. Zeng, C. Qi, S. Lu, J. Xu, C. Zhao, Z. Dong, C. Lei, Hydrophobic association and ionic coordination dual crossed-linked conductive hydrogels with self-adhesive and self-healing virtues for conformal strain sensors. *J. Polym. Sci.* **60**, 812–824 (2021).
158. X. Li, Z. Liu, Y. Liang, L. M. Wang, Y. D. Liu, Chitosan-based double cross-linked ionic hydrogels as a strain and pressure sensor with broad strain-range and high sensitivity. *J. Mater. Chem. B* **10**, 3434–3443 (2022).
159. J. Wang, T. Dai, H. Wu, M. Ye, G. Yuan, H. Jia, Tannic acid-Fe^{3+} activated rapid polymerization of ionic conductive hydrogels with high mechanical properties, self-healing, and self-adhesion for flexible wearable sensors. *Compos. Sci. Technol.* **221**, 109345 (2022).
160. Q. Zeng, S. Wan, S. Yang, X. Zhao, F. He, Y. Zhang, X. Cao, Q. Wen, Y. Feng, G. Yu, L. Pan, J. Li, Super stretchability, strong adhesion, flexible sensor based on Fe^{3+} dynamic coordination sodium alginate/polyacrylamide dual-network hydrogel. *Colloids Surf. A Physicochem. Eng. Asp.* **652**, 129733 (2022).
161. H. Fu, B. Wang, J. Li, J. Xu, J. Li, J. Zeng, W. Gao, K. Chen, A self-healing, recyclable and conductive gelatin/nanofibrillated cellulose/Fe^{3+} hydrogel based on multi-dynamic interactions for a multifunctional strain sensor. *Mater. Horiz.* **9**, 1412–1421 (2022).
162. L. Zou, B. Chang, H. Liu, X. Zhang, H. Shi, X. Liu, E. Euchler, C. Liu, Multiple physical bonds cross-linked strong and tough hydrogel with antibacterial ability for wearable strain sensor. *ACS Appl. Polym. Mater.* **4**, 9194–9205 (2022).
163. X. Sun, H. Wang, Y. Ding, Y. Yao, Y. Liu, J. Tang, Fe^{3+}-Coordination mediated synergistic dual-network conductive hydrogel as a sensitive and highly-stretchable strain sensor with adjustable mechanical properties. *J. Mater. Chem. B* **10**, 1442–1452 (2022).
164. Y. Liu, Z. Zhang, Z. Liang, Y. Yong, C. Yang, Z. Li, Multifunctional polyurethane hydrogel based on a phenol-carbamate network and an Fe^{3+}-polyphenol coordination bond toward NIR light triggered actuators and strain sensors. *J. Mater. Chem. A* **10**, 16928–16940 (2022).
165. Y. Liu, Y. Liu, Z. Yang, X. Chen, Y. Zhao, Preparation of MPASP-PAA/Fe^{3+} composite conductive hydrogel with physical and chemical double crosslinking structure and its application in flexible strain sensors. *Macromol. Chem. Phys.* **223**, 2100467 (2022).
166. Y. Song, L. Niu, P. Ma, X. Li, J. Feng, Z. Liu, Rapid preparation of antifreezing conductive hydrogels for flexible strain sensors and supercapacitors. *ACS Appl. Mater. Interfaces* **15**, 10006–10017 (2023).
167. Q. Pang, H. Hu, H. Zhang, B. Qiao, L. Ma, Temperature-responsive ionic conductive hydrogel for strain and temperature sensors. *ACS Appl. Mater. Interfaces* **14**, 26536–26547 (2022).
168. A. Maitra, S. Paria, S. K. Karan, R. Bera, A. Bera, A. K. Das, S. K. Si, L. Halder, A. De, B. B. Khatua, Triboelectric nanogenerator driven self-charging and self-healing flexible asymmetric supercapacitor power cell for direct power generation. *ACS Appl. Mater. Interfaces* **11**, 5022–5036 (2019).
169. R. Yuan, N. Yang, S. Fan, Y. Huang, D. You, J. Wang, Q. Zhang, C. Chu, Z. Chen, L. Liu, L. Ge, Biomechanical motion-activated endogenous wound healing through LBL self-powered nanocomposite repairer with pH-responsive anti-inflammatory effect. *Small* **17**, e2103997 (2021).
170. Q. Gao, C. Li, M. Wang, J. Zhu, D. R. Munna, P. Wang, C. Zhu, J. Gao, C. Gao, A highly adhesive, self-healing and perdurable PEDOT:PSS/PAA–Fe^{3+} gel enabled by multiple non-covalent interactions for multi-functional wearable electronics. *J. Mater. Chem. C* **10**, 6271–6280 (2022).
171. Y. Feng, J. Yu, D. Sun, C. Dang, W. Ren, C. Shao, R. Sun, Extreme environment-adaptable and fast self-healable eutectogel triboelectric nanogenerator for energy harvesting and self-powered sensing. *Nano Energy* **98**, 107284 (2022).
172. Y. Luo, M. Yu, Y. Zhang, Y. Wang, L. Long, H. Tan, N. Li, L. Xu, J. Xu, Highly sensitive strain sensor and self-powered triboelectric nanogenerator using a fully physical crosslinked double-network conductive hydrogel. *Nano Energy* **104**, 107955 (2022).
173. L. Wang, W. A. Daoud, Hybrid conductive hydrogels for washable human motion energy harvester and self-powered temperature-stress dual sensor. *Nano Energy* **66**, 104080 (2019).
174. M. Yang, X. Tian, T. Hua, Transparent, stretchable, and adhesive conductive ionic hydrogel-based self-powered sensors for smart elderly care systems. *ACS Appl. Mater. Interfaces* **15**, 11802–11811 (2023).
175. X. Jing, H. Li, H. Y. Mi, P. Y. Feng, X. Tao, Y. Liu, C. Liu, C. Shen, Enhancing the performance of a stretchable and transparent triboelectric nanogenerator by optimizing the hydrogel ionic electrode property. *ACS Appl. Mater. Interfaces* **12**, 23474–23483 (2020).
176. B. Ying, R. Zuo, Y. Wan, X. Liu, An ionic hydrogel-based antifreezing triboelectric nanogenerator. *ACS Appl. Electron. Mater.* **4**, 1930–1938 (2022).
177. K. T. Huang, K. Ishihara, C. J. Huang, Polyelectrolyte and antipolyelectrolyte effects for dual salt-responsive interpenetrating network hydrogels. *Biomacromolecules* **20**, 3524–3534 (2019).
178. J. Shen, M. Du, Z. Wu, Y. Song, Q. Zheng, Strategy to construct polyzwitterionic hydrogel coating with antifouling, drag-reducing and weak swelling performance. *RSC Adv.* **9**, 2081–2091 (2019).
179. L. Sun, S. Chen, Y. Guo, J. Song, L. Zhang, L. Xiao, Q. Guan, Z. You, Ionogel-based, highly stretchable, transparent, durable triboelectric nanogenerators for energy harvesting and motion sensing over a wide temperature range. *Nano Energy* **63**, 103847 (2019).
180. Z. Wang, J. Chen, L. Wang, G. Gao, Y. Zhou, R. Wang, T. Xu, J. Yin, J. Fu, Flexible and wearable strain sensors based on tough and self-adhesive ion conducting hydrogels. *J. Mater. Chem. B* **7**, 24–29 (2019).
181. B. Yang, W. Yuan, Highly stretchable, adhesive, and mechanical zwitterionic nanocomposite hydrogel biomimetic skin. *ACS Appl. Mater. Interfaces* **11**, 40620–40628 (2019).
182. L. Wang, G. Gao, Y. Zhou, T. Xu, J. Chen, R. Wang, R. Zhang, J. Fu, Tough, adhesive, self-healable, and transparent ionically conductive zwitterionic nanocomposite hydrogels as skin strain sensors. *ACS Appl. Mater. Interfaces* **11**, 3506–3515 (2019).
183. H. Yin, D. R. King, T. L. Sun, Y. Saruwatari, T. Nakajima, T. Kurokawa, J. P. Gong, Polyzwitterions as a versatile building block of tough hydrogels: From polyelectrolyte complex gels to double-network gels. *ACS Appl. Mater. Interfaces* **12**, 50068–50076 (2020).
184. X. Pei, H. Zhang, Y. Zhou, L. Zhou, J. Fu, Stretchable, self-healing and tissue-adhesive zwitterionic hydrogels as strain sensors for wireless monitoring of organ motions. *Mater. Horiz.* **7**, 1872–1882 (2020).
185. J. Zhang, L. Chen, B. Shen, J. Mo, F. Tang, J. Feng, Highly stretchable and self-healing double network hydrogel based on polysaccharide and polyzwitterion for wearable electric skin. *Polymer* **194**, 122381 (2020).
186. X. Jin, H. Jiang, F. Qiao, W. Huang, X. Bao, Z. Wang, Q. Hu, Fabrication of alginate-P(SBMA-co-AAm) hydrogels with ultrastretchability, strain sensitivity, self-adhesiveness, biocompatibility, and self-cleaning function for strain sensors. *J. Appl. Polym. Sci.* **138**, 49697 (2020).
187. D. Zhang, Y. Tang, Y. Zhang, F. Yang, Y. Liu, X. Wang, J. Yang, X. Gong, J. Zheng, Highly stretchable, self-adhesive, biocompatible, conductive hydrogels as fully polymeric strain sensors. *J. Mater. Chem. A* **8**, 20474–20485 (2020).
188. C. Wen, H. Guo, J. Yang, Q. Li, X. Zhang, X. Sui, M. Cao, L. Zhang, Zwitterionic hydrogel coated superhydrophilic hierarchical antifouling floater enables unimpeded interfacial steam generation and multi-contamination resistance in complex conditions. *Chem. Eng. J.* **421**, 130344 (2021).
189. S. Xiao, X. He, Z. Zhao, G. Huang, Z. Yan, Z. He, Z. Zhao, F. Chen, J. Yang, Strong anti-polyelectrolyte zwitterionic hydrogels with superior self-recovery, tunable surface friction, conductivity, and antifreezing properties. *Eur. Polym. J.* **148**, 110350 (2021).
190. M. Qiu, H. Liu, B. Tawiah, H. Jia, S. Fu, Zwitterionic triple-network hydrogel electrolyte for advanced flexible zinc ion batteries. *Compos. Commun.* **28**, 100942 (2021).

191. J. Yang, Z. Xu, J. Wang, L. Gai, X. Ji, H. Jiang, L. Liu, Antifreezing zwitterionic hydrogel electrolyte with high conductivity of 12.6 mS cm^{-1} at −40 °C through hydrated lithium ion hopping migration. *Adv. Funct. Mater.* **31**, 2009438 (2021).
192. S. Y. Zheng, S. Mao, J. Yuan, S. Wang, X. He, X. Zhang, C. Du, D. Zhang, Z. L. Wu, J. Yang, Molecularly engineered zwitterionic hydrogels with high toughness and self-healing capacity for soft electronics applications. *Chem. Mater.* **33**, 8418–8429 (2021).
193. Z. Zhou, Z. He, S. Yin, X. Xie, W. Yuan, Adhesive, stretchable and antibacterial hydrogel with external/self-power for flexible sensitive sensor used as human motion detection. *Compos. B Eng.* **220**, 108984 (2021).
194. H. Wei, Z. Wang, H. Zhang, Y. Huang, Z. Wang, Y. Zhou, B. B. Xu, S. Halila, J. Chen, Ultrastretchable, highly transparent, self-adhesive, and 3D-printable ionic hydrogels for multimode tactical sensing. *Chem. Mater.* **33**, 6731–6742 (2021).
195. W. Zhang, F. Guo, H. Mi, Z. S. Wu, C. Ji, C. Yang, J. Qiu, Kinetics-boosted effect enabled by zwitterionic hydrogel electrolyte for highly reversible zinc anode in zinc-ion hybrid micro-supercapacitors. *Adv. Energy Mater.* **12**, 2202219 (2022).
196. T. Wu, C. Ji, H. Mi, F. Guo, G. Guo, B. Zhang, M. Wu, Construction of zwitterionic osmolyte-based hydrogel electrolytes towards stable zinc anode for durable aqueous zinc ion storage and integrated electronics. *J. Mater. Chem. A* **10**, 25701–25713 (2022).

Acknowledgments

Funding: S.C.T. acknowledges the Ministry of Education Singapore Academic Research Fund (Tier 2 grant no. A-0005415-01-00). S.Z. acknowledges the support from the National Natural Science Foundation of China (52403156), Science and Technology Commission of Shanghai Municipality (24ZR1406700 and 24PJA010), and Fudan University (JIH2328001Y). R.W. and X.H. acknowledge the National Natural Science Foundation of China (no. 52403156). **Author contributions:** X.G. conceived the idea and designed the experiments. S.C.T., S.Z., R.W., X.H., Z.Wang, and C.Y. supervised the project. X.G., S.P., X.S., and Z.Wei performed the experiments and contributed to the data analysis. Y.-L.Z. conducted the theoretical calculations. X.G., S.P., and S.Z. wrote and revised the manuscript. All authors discussed the research and reviewed the manuscript before submission. **Competing interests:** The authors declare that they have no competing interests. **Data and materials availability:** All data needed to evaluate the conclusions in the paper are present in the paper and/or the Supplementary Materials.

Submitted 9 January 2025
Accepted 15 April 2025
Published 16 May 2025
10.1126/sciadv.adv8523